J Muscle Res Cell Motil (2010) 31:13–33
DOI 10.1007/s10974-009-9195-8

ORIGINAL PAPER

Effects of membrane depolarization and changes in extracellular $[K^+]$ on the Ca^{2+} transients of fast skeletal muscle fibers. Implications for muscle fatigue

Marbella Quiñonez · Fernando González · Consuelo Morgado-Valle · Marino DiFranco

Received: 31 August 2009 / Accepted: 11 December 2009 / Published online: 5 January 2010

Abstract Repetitive activation of skeletal muscle fibers leads to a reduced transmembrane K^+ gradient. The resulting membrane depolarization has been proposed to play a major role in the onset of muscle fatigue. Nevertheless, raising the extracellular K^+ (K_o^+) concentration ($[K^+]_o$) to 10 mM potentiates twitch force of rested amphibian and mammalian fibers. We used a double Vaseline gap method to simultaneously record action potentials (AP) and Ca^{2+} transients from rested frog fibers activated by single and tetanic stimulation (10 pulses, 100 Hz) at various $[K^+]_o$ and membrane potentials. Depolarization resulting from current injection or raised $[K^+]_o$ produced an increase in the resting $[Ca^{2+}]$. Ca^{2+} transients elicited by single stimulation were potentiated by depolarization from −80 to −60 mV but markedly depressed by further depolarization. Potentiation was inversely correlated with a reduction in the amplitude, overshoot and duration of APs. Similar effects were found for the Ca^{2+} transients elicited by the first pulse of 100 Hz trains. Depression or block of Ca^{2+} transient in response to the 2nd to 10th pulses of 100 Hz trains was observed at smaller depolarizations as compared to that seen when using single stimulation. Changes in Ca^{2+} transients along the trains were associated with impaired or abortive APs. Raising $[K^+]_o$ to 10 mM potentiated Ca^{2+} transients elicited by single and tetanic stimulation, while raising $[K^+]_o$ to 15 mM markedly depressed both responses. The effects of 10 mM K_o^+ on Ca^{2+} transients, but not those of 15 mM K_o^+, could be fully reversed by hyperpolarization. The results suggests that the force potentiating effects of 10 mM K_o^+ might be mediated by depolarization dependent changes in resting $[Ca^{2+}]$ and Ca^{2+} release, and that additional mechanisms might be involved in the effects of 15 mM K_o^+ on force generation.

Keywords Muscle fatigue · Potassium · Membrane potential · Excitation–contraction coupling · Calcium release · High frequency stimulation

M. Quiñonez · F. González · M. DiFranco
Laboratorio de Fisiología y Biofisíca del Músculo, IBE, UCV, Caracas, Venezuela
e-mail: mquinonez@mednet.ucla.edu

F. González
e-mail: fernando.gonzalez@ciens.ucv.ve

C. Morgado-Valle
Programa de Neurobiologia, Universidad Veracruzana, Veracruz, México
e-mail: consuelomorgado@yahoo.com

M. Quiñonez · M. DiFranco (✉)
Department of Physiology, David Geffen School of Medicine, UCLA, Los Angeles, CA 90024, USA
e-mail: mdifranco@mednet.ucla.edu

Introduction

When skeletal muscles are stimulated repetitively their mechanical output decreases progressively with time. This phenomenon is known as muscle fatigue (Edwards 1981). Although its etiology is not yet completely understood, fatigue can be demonstrated in intact isolated fibers (for a review, see Westerblad and Allen 2003; Allen et al. 2008). This finding overrules the possibility that changes in the CNS or the neuromuscular junction are the cause of muscle fatigue and demonstrates instead that it has a myogenic origin (Bigland-Ritchie and Woods 1984). The extent and time course of the development of, and the recovery from, muscle fatigue depend, among other factors, on the pattern of stimulation and fiber type. For fast fibers, continuously

stimulated at high frequency, fatigue most likely results from changes in the mechanisms underlying electrical excitability and the coupling between APs and Ca^{2+} release (Grabowski et al. 1972; Gonzalez-Serratos et al. 1978; Lannergren and Westerblad 1986).

Changes in trans-sarcolemmal K^+ and Na^+ gradients resulting from ionic fluxes during prolonged stimulation have been proposed to be at the root of high frequency fatigue (Juel 1986). In particular, large changes in $[K^+]_o$ (including the muscle interstitium and the blood) and intracellular K^+ concentration ($[K^+]_i$) has been measured from working muscles in vivo (Sjogaard et al. 1985; Balog and Fitts 1996; Juel et al. 2000; Nordsborg et al. 2003). Recently, it has been calculated that $[K^+]_o$ can reach values as high as 26–52 mM depending on fiber type (Clausen 2008). Based on the complex architecture of the transverse tubular system, it has also been proposed that K^+ accumulation might be larger in the lumen of the *t*-tubules than in the interstitium or the plasma (Fitts 1994; Shorten et al. 2007; Cairns and Lindinger 2008). It is also expected that the magnitude of changes in luminal $[K^+]$ and AP features varies along the fiber's radius. In extreme situations, the inner segments of the *t*-tubules might become unexcitable, and Ca^{2+} release abolished. *Ex vivo* it has been largely demonstrated that increasing $[K^+]_o$ lead to fiber depolarization and reduction in force development in both amphibian and mammalian muscles (Renaud and Light 1992; Cairns et al. 1995, 1997); for recent reviews see (Allen et al. 2008; Kristensen and Juel 2009). According to the "potassium hypothesis" for muscle fatigue (Renaud and Light 1992), membrane depolarization resulting from extracellular K^+ accumulation (and intracellular K^+ loss) during continuous activation would be the major cause of fatigue. Membrane depolarization per se would reduce the availability of Na^+ channels and the Na^+ electromotive force. As a consequence, the amplitude, overshoot and speed of the rising phase of the AP would be reduced. It is expected that those impairments in AP would lead to a smaller Ca^{2+} release, which in turn will result in a reduced active force generation. Nevertheless, several mechanisms have been suggested to act in vivo to prevent the loss of excitability during voluntary exercise (for a review see Allen et al.).

Similarly, according to the "sodium hypothesis" for muscle fatigue (Cairns et al. 2003), the sodium concentration ($[Na^+]$) is expected to decrease in the *t*-tubule lumen and to increase in the myoplasm upon repetitive stimulation (Juel 1986). Several lines of evidence support that such changes can impair AP conduction along the *t*-tubules (Bezanilla et al. 1972; Duty and Allen 1994). In addition, the effects of changes in the transmembrane gradients of both ions have been suggested to be synergistic rather than being additive (Bouclin et al. 1995).

One approach to test the potassium hypothesis *ex vivo* is to study the effects of raising the $[K^+]_o$ on rested intact fibers while keeping constant all other factors potentially involved in muscle fatigue (Renaud and Light 1992; Cairns et al. 2003). Using this paradigm, it has been demonstrated that rising $[K^+]_o$ has differential concentration-dependent effects on twitch and tetanic force. Increasing $[K^+]_o$ up to 10 mM has no effect on tetanic force but, unexpectedly, potentiates twitch force. Further increase in $[K^+]_o$ to 15 mM depresses both twitch and tetanic force (Renaud and Light 1992; Cairns et al. 1997). The mechanisms underlying these effects are not known. Impairment of Ca^{2+} release has been suggested as a possible mechanism underlying force generation depression in response to raised $[K^+]_o$ (Renaud and Light 1992), but this possibility has not been yet tested.

To further investigate the potassium hypothesis; here we used rested cut fibers as an alternative model to intact fibers. Fibers were mounted on a Vaseline gap chamber (DiFranco et al. 1999; Quinonez and DiFranco 2000), stretched to sarcomeric lengths of about 4 μm and loaded with a low affinity Ca^{2+} dye. In these conditions, fiber shortening is prevented without significantly altering the endogenous buffering capacity of the fibers, and electrical responses and Ca^{2+} transients elicited by single and tetanic stimulation could be simultaneously detected without distortion. In addition, the method allows for fast changes in the $[K^+]_o$ and to control the steady state membrane potential by current injection, thus permitting the study of the effects of changing each parameter in isolation.

The aims of this study were to determine the effects of rising $[K^+]_o$ on electrical excitability and Ca^{2+} release and whether these effects could be reproduced by depolarization at normal $[K^+]_o$, or reversed by hyperpolarization at raised $[K^+]_o$.

We found that raising $[K^+]_o$ to 10 mM results in membrane depolarization, reduction of AP amplitude and overshoot, and potentiation of Ca^{2+} transients elicited by single and 100 Hz stimulation. These effects could be mimicked and, more importantly, reversed by current injection. The effects of depolarization (induced by current injection) on Ca^{2+} transients were remarkably similar to the previously reported effects of raising $[K^+]_o$ on twitch tension. Ca^{2+} transients elicited by single and tetanic stimulation were depressed in fibers exposed to 15 mM K_o^+. This changes were reversed by reducing $[K^+]_o$ to 2.5 mM but not by fiber hyperpolarization. The results suggest that the effects of 10 mM K_o^+, but not 15 mM K_o^+, on force generation can be mostly explained by changes in Ca^{2+} release produced by fiber depolarization.

A similar study on the effects of reducing $[Na^+]_o$ at different membrane potentials will be published elsewhere. Part of this work was presented in abstract form (Quiñonez et al. 2009).

Methods

Animal model

Animals were handled in accordance to the regulations laid down by Universidad Central de Venezuela. Anesthetized animals were killed by rapid transection of the cervical spinal cord, followed by pithing in the cranial and caudal directions. Experiments were performed with segments of fibers dissected from the dorsal head of the semitendinosus muscle of tropical toads (Leptodactilus sp.).

Solutions

All the solutions, which composition (in mM) is shown below, were adjusted to a pH = 7.2 and an osmolarity of 250 mOsmol/kg H_2O. Ringer solution: 115 NaCl, 2.5 KCl, 1.8 $CaCl_2$, 1 $MgCl_2$ and 10 MOPS (4-morpholineethanesulfonic acid); titrated with NaOH. In order to make our results comparable to those obtained in studies of the effects of raised $[K^+]_o$ on the mechanical output of rested muscles (Renaud and Light 1992; Cairns et al. 1997); Ringer solutions with higher $[K^+]$ (10 and 15 mM) were made by equimolar exchange of NaCl with KCl, as reported previously (Renaud and Light 1992). Saturation solution: 80 $CaCl_2$, 10 MOPS; titrated with NaOH. Internal solution: 110 aspartate, 5 K_2-ATP, 5 Na_2-creatine phosphate, 20 MOPS, 0.1 EGTA (ethylene glycol tetraacetic acid), 5 $MgCl_2$, 0.5 mg/ml creatine phosphokinase; titrated with KOH. All chemicals were from Sigma (St. Louis, Missouri, USA); Ca^{2+} dyes were from Molecular Probes (Invitrogen, Carlsbad, California, USA).

Electrophysiological techniques

Cut skeletal muscle fibers were mounted in an inverted double Vaseline gap chamber and maintained in current clamp conditions as previously described (DiFranco et al. 1999). Briefly, the segment of fiber was divided in three electrically isolated sections by two vacuum grease (Glisseal, Borer Chemie, Zuchwil, Switzerland; DiFranco et al. 1999) seals. The electrical and optical measurements were made at the central section, ~500 μm in length. The lateral fiber sections were permeabilized using saponin (0.1 mg/ml) to improve the exchange of solutes between the internal solution contained in the chamber's lateral pools and the myoplasm of the central section of the fiber. Fibers were stretched to a sarcomere spacing of 4–4.5 μm to prevent movement dependent optical artifacts. The sarcomere spacing was measured from images acquired with a 100× 1.3NA objective and a CCD camera (Spectrasource, CA, USA). At the beginning of the experiments the membrane potential was adjusted to −100 mV ("resting potential") and then varied to values between −100 and −55 mV by current injection through one of the cut ends. A 3 min period was allowed after changing the membrane potential. Single pulses or short trains of pulses (100 Hz, 10 pulses) were used to trigger action potentials (APs), which in turn elicited calcium release. Pulse duration was 0.2 ms, and amplitude was adjusted to ~15% above the threshold at −100 mV, and not changed thereafter. The central pool was continuously perfused with external solution. The perfusion system had a dead time of ~2 s. A 20 min period was allowed for equilibration after changing solutions. Experiments were performed at room temperature (~20°C).

Calcium measurement

Steady myoplasmic $[Ca^{2+}]$ and AP elicited myoplasmic $[Ca^{2+}]$ changes were followed with the low affinity fluorescent calcium dye Oregon green 488 BAPTA 5N (OGB5N) and the high affinity dyes Fluo-3 and Rhod-2. The dyes were dissolved in the internal solution and loaded into the fibers through the cut ends. After mounting the fibers, a 30 min period was allowed for equilibration between the end pools and the central section of the fiber. The chamber was mounted on the stage of an inverted microscope (Diaphot, Nikon Instruments Inc., Melville, New York, USA) equipped with a standard epifluorescence attachment. A mercury arc lamp was used as the light source. A 2B-A fluorescence cube (Nikon, 490//505//520–560, in nm, excitation/dichroic/emission, respectively) was used to separate excitation and emission wavelengths for Fluo-3 and OGB-5N. A G-1B cube (Nikon, 510–551//565//590, in nm) was used for Rhod-2. Dye excitation periods were kept as short as possible and synchronized to the electrical stimulation using a lab-made electromagnetic shutter under computer command. In most cases, myoplasmic $[Ca^{2+}]$ changes are presented in molar units calculated from the Ca^{2+} dependent fluorescence changes using the following expression:

$$[Ca^{2+}]_t = \frac{\left[[Ca^{2+}]_{rest} + (F_{max} - F_{rest}) \cdot K_d\right] + [(\Lambda F \cdot K_d) + dF/F]}{(F_{max} - F_{rest} - \Lambda F) \cdot K_d} \quad (1)$$

(Caputo et al. 1994), where: $[Ca^{2+}]_t$ is the change of free myoplasmic calcium concentration with time (referred thereafter as a "calcium transient"), F_{max} is the dye fluorescence at saturating $[Ca^{2+}]$, $[Ca^{2+}]_{rest}$ is the free $[Ca^{2+}]$ at rest, K_d is the dye-calcium complex dissociation constant, and ΔF is the fluorescence change above the resting level, calculated as $F_t - F_{rest}$, and dF/F is the time derivative of ΔF. $[Ca^{2+}]_{rest}$ was taken as 100 nM (Lopez et al. 1983), although it should be noted that there is no general agreement about the $[Ca^{2+}]_{rest}$ in skeletal muscle

fibers. Reported values vary widely between <50 and >300 nM (Lopez et al. 1983; Blatter and Blinks 1991; Kurebayashi et al. 1993), probably depending on the method used. We consider the value initially determined with Ca^{2+} sensitive electrodes (e.g. 100 nM; Lopez et al. 1983) as a reasonable compromise among published values. This value of 100 nM for the $[Ca^{2+}]_{rest}$, has been previously used for the same kind of calculations performed here (Caputo et al. 1994); and more recently the same value, but calculated from Fura-2 fluorescence measurements, has been assumed by others for mouse skeletal muscle (Lynch et al. 1997). F_t and F_{rest} are the fluorescence as a function of time and the resting fluorescence, respectively. K_ds were calculated from saturation curves generated from cuvette measurements. To this end, Ca^{2+} dyes were dissolved (10 μM) in solutions of known pCa's (CALBUF-2, WPI, Sarasota, Florida, USA) and the fluorescence measured in the same setup used for electrophysiological and optical experiments (DiFranco et al. 1999). Published Ca^{2+} dyes parameters used for Ca^{2+} transient calculations are given in Table 1 (Caputo et al. 1994; Escobar et al. 1997; DiGregorio et al. 1999). F_{max} was measured at the end of some experiments using a method similar to that previously described (DiFranco 1991; Sanchez and Vergara 1994). Briefly, the fibers were exposed to an isotonic Ca^{2+} solution containing 0.1 mg/ml saponin (see "Solutions"). Differing from the previous method (DiFranco 1991), however, fixatives were not used since it was found that stretching the fibers to 4–4.5 μm sufficed to prevent contraction in the presence of saturating $[Ca^{2+}]$ for a period longer than that needed to reach dye saturation. Figure 1 shows an example of a saturation experiment. It can be seen that soon after applying the saturating solution (arrow) the fluorescence increased monotonically to a maximum (F_{max}), and then decreased more slowly to a level below that observed before exposure to saturation solution (Fig. 1A). In addition, it should be noted that, the fluorescence changes are preceded by fiber depolarization (Fig. 1B). In all certainty, the increase in fluorescence is due to the influx of calcium into the fiber, whereas the later decay is due to washout of the dye-calcium complex out of the fiber. The average F_{max} for the three dyes are given in Table 1. For comparison, a fluorescence transient was elicited by AP stimulation prior to the saturation procedure (Fig. 1A, B), and the calculated Ca^{2+} transient is shown in the inset in Fig. 1A. In some cases, calcium dependent fluorescence transients were expressed as dimensionless fractional fluorescence changes ($\Delta F/F = (F_t - F_{rest})/F_{rest}$); referred thereafter as "fluorescence transients".

Data acquisition and analysis

Membrane potential and fluorescence were filtered at 5 and 2 kHz, repectively, using 8-pole Bessel filters (Frequency Devices, Ottawa, Illinois, USA); and acquired simultaneously using a Digidata 1200A acquisition board and Axotape software (Molecular Devices, Sunnyvale, California, USA). Data were analyzed using Origin 6.0 (Origin Microcal, Northampton, Massachusetts, USA). Data are presented as mean ± SE. Significance was set at $P < 0.05$.

Table 1 Parameters of calcium dyes

Dye	K_{on} (μM^{-1}. ms^{-1})	K_{off} (ms^{-1})	K_d (μM)	F_{max}/F_{rest} (mean ± SE)	References
OGB-5N	0.17	5.6	32.9	13.2 ± 0.87 ($n = 6$)	DiGregorio et al. (1999)
Fluo-3	0.03	0.12	4.0	17.5 ± 3.9 ($n = 4$)	Caputo et al. (1999)
Rhod-2	0.069	0.13	1.87	22.6 ± 5.6 ($n = 4$)	Escobar et al. (1997)

K_{on} y K_{off} are the on and off rate constants, respectively. K_d is the dissociation constant. F_{rest} and F_{max} are the dye fluorescence measured in vivo in fibers at rest or exposed to saturating $[Ca^{2+}]$. n is the number of measurements

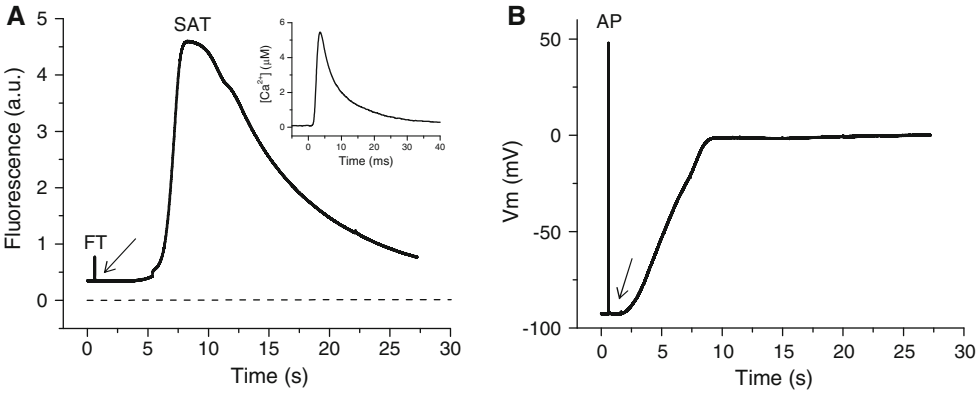

Fig. 1 Measurement of F_{max} in live fibers. **A** Fluorescence transient (*FT*) elicited by AP stimulation and fluorescence changes (*SAT*) in response to exposure to the saturation solution (*arrow*). The *inset* shows the Ca^{2+} transient calculated from the fluorescence transient. **B** Action potential (*AP*) and transmembrane potential changes in response to exposure to the saturation solution (*arrow*)

Results

Ca^{2+} transients calculated from fibers loaded with different fluorescent dyes and stretched to different sarcomere length

We first verified the usefulness of high- (Rhod-2 and Fluo-3) and low affinity (OGB-5N) Ca^{2+} dyes to track fast Ca^{2+} transients elicited by single APs or short trains of APs, and determined the minimal fiber stretching assuring the effective prevention of possible mechanical artifacts in the presence of low EGTA concentrations ([EGTA]). Fluorescence transients from the 3 dyes, obtained in similar conditions in response to single stimulation, are shown superimposed in Fig. 2A. A normalized scale is used to highlight the kinetics differences among the fluorescence transients. As expected from their K_ds, the slower and faster transients were recorded from fibers loaded with Rhod-2 and OGB-5N, respectively; whereas transients from fibers loaded with Fluo-3 displayed intermediate kinetics. See Table 2 for comparative kinetic parameters. Ca^{2+} transients calculated from fluorescence transients in Fig. 2A are

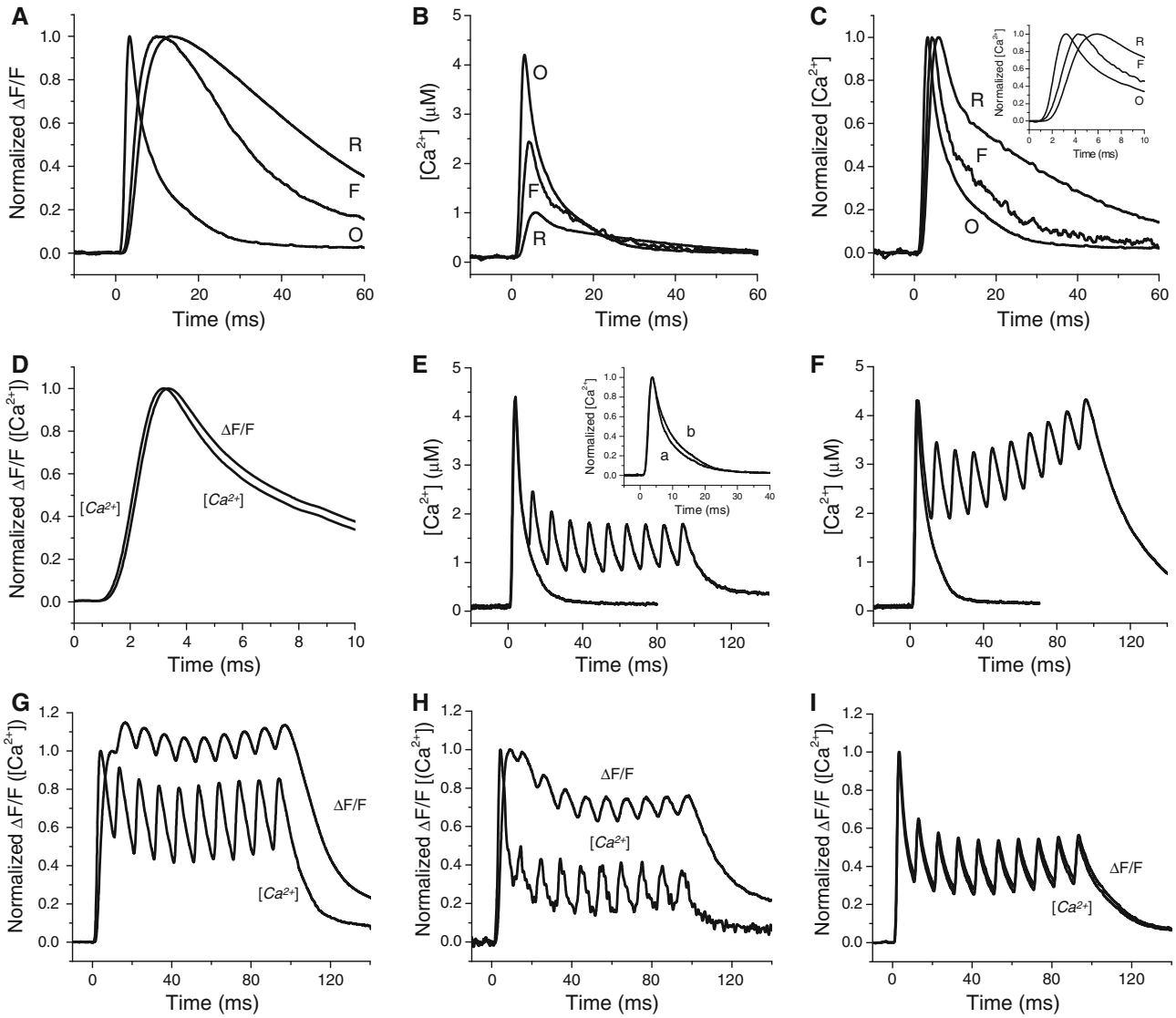

Fig. 2 Ca^{2+} transients calculated from fibres loaded with different Ca^{2+} dyes and stretched to different sarcomere lengths. **A** Normalized fluorescence transients from fibers loaded with Rhod-2 (*R*), Fluo-3 (*F*) and OGB-5N(O). **B** Ca^{2+} transients calculated from the data in **A**. **C** Normalized Ca^{2+} transients from **B**. The *inset* in **C** shows the same transients in an expanded time scale. **D** Comparison of fluorescence ($\Delta F/F$) and Ca^{2+} transients ($[Ca^{2+}]$) from a fibre loaded with OGB-5N. **E** Ca^{2+} transients calculated from OGB-5N transient from a fiber stretched at 4.5 μm and stimulated with a single pulse and a train of pulses. **F** Ca^{2+} transients calculated from OGB-5N transient from a fiber stretched at 3.6 μm and stimulated with a single pulse and a train of pulses. The inset in panel E compares Ca^{2+} transients shown in **E** (trace a) and **F** (trace b). **G–I**. Ca^{2+} and fluorescence transients elicited by 100 Hz stimulation in fibers loaded with Rhod-2 (**G**), Fluo-3 (**H**) and OGB-5N (**I**). Sarcomere length: 4.5 μm (**A–E**, **G–I**) and 3.6 μm (**F**)

Table 2 Amplitude and kinetic parameters of Ca^{+2} transients calculated from OGB-5N, Fluo-3 and Rhod-2 fluorescence transients

Dye	Delay (ms)	T_{peak} (ms)	$d[Ca^{+2}]/dt_{max}$ (μM ms^{-1})	FDHM (ms)	Amplitude (μM)	Peak $\Delta F/F$
OGB-5N ($n = 12$)	0.83 ± 0.01	3.19 ± 0.03	3.2 ± 0.01	4.82 ± 0.02	4.48 ± 0.26	1.68 ± 0.09
Fluo-3 ($n = 10$)	0.88 ± 0.02	4.2 ± 0.04	1.61 ± 0.07	6.8 ± 0.4	2.66 ± 0.19	2.4 ± 0.25
Rhod-2 ($n = 12$)	0.94 ± 0.02	4.38 ± 0.05	0.9 ± 0.08	8.43 ± 0.37	1.53 ± 0.09	10.2 ± 0.52

Delay is the coupling delay between the AP and Ca^{2+} transient onsets. T_{peak} is the time to peak of the Ca^{2+} transient. $d[Ca^{+2}]/dt_{max}$ is the maximun derivative of the raising phase of Ca transients. FDHM is the duration at half maximun ot the Ca^{2+} transient. Amplitude is the amplitude of the Ca^{2+} transient. Peak $\Delta F/F$ is the peak value of the fractional fluorescence transiets. Values are mean ± SE. n is the number of measurements

shown in Fig. 2B and C. Ca^{2+} transients calculated from Rhod-2 and Fluo-3 transients display a remarkable "kinetic correction", and approach the time course of Ca^{2+} transients calculated from OGB-5N transients, which reported the faster and larger free $[Ca^{2+}]$ changes. In addition to its kinetic limitation, and unexpectedly for a single binding site dye, Ca^{2+} transients from Rhod-2 display a two time constant decay. This behavior is in contrast to that found for Fluo-3 and OGN-5N, which display a monotonic decaying phase. The parameters characterizing Ca^{2+} transient calculated with Eq. 1 from fluorescence transients of the 3 dyes are shown in Table 2. The superiority of OGB-5N to track fast $[Ca^{2+}]$ changes is further stressed by superimposing fluorescence and Ca^{2+} data. As can be seen in Fig. 2D, Ca^{2+} transients are only slightly faster than OGB-5N fluorescence transients. This results from an acceleration of both the rising and falling phases, and a reduction of the time to peak of the Ca^{2+} transients as compared with the parameters of the corresponding fluorescence transient. This result suggests that at room temperature the reaction between OGB-5N and Ca^{2+} is close to equilibrium during the Ca^{2+} release.

We found that, in order to obtain a faithful portrait of Ca^{2+} release when using low EGTA concentrations and high frequency Stimulation, fibers should be stretched to about 4 μm. Figure 2E and F compare Ca^{2+} transients calculated from OGB-5N transients obtained from 2 fibers loaded with 100 μM EGTA and stretched to 4.5 and 3.6 μm, respectively. As can be seen from the inset in Fig. 2E, responses to single stimulation obtained from both sarcomere lengths are closely similar, discarding any deleterious effect of stretching on Ca^{2+} release (see also DiFranco et al. 2002). Nevertheless, different responses are seen when using short high frequency (i.e. 100 Hz) trains. While in highly stretched fibers (Fig. 2E) peak Ca^{2+} release decays monotonically in response to the first 3–4 pulses towards a relatively steady value afterwards, a staircase response starting after the second pulse response is seen in less stretched fibers (Fig. 2F). As expected from single stimulation data, comparison of fluorescence and Ca^{2+} data obtained from fibers stretched to ~4 μm and stimulated at 100 Hz (Fig. 2G–I) shows that Ca^{2+} dyes with very high K_ds are not appropriate to study Ca^{2+} release in fast muscle fibers in response to high frequency stimulation (Baylor and Hollingworth 2003). The similarity in the kinetics of Ca^{2+} data in Fig. 2H and I reinforces the usefulness of Eq. 1 to calculate Ca^{2+} transients and the need for the effective restriction of fiber contraction in order to faithfully study Ca^{2+} release. In addition, they show the limitations of optical studies of Ca^{2+} release performed in contracting fibers loaded with high affinity dyes.

Calcium handling in fibers polarized at various membrane potentials

Since the increase in $[K^+]_o$ is known to cause a reduction in membrane potential, we first studied the effects of the membrane depolarization on calcium handling in the presence of physiological $[K^+]_o$. To this end, appropriate steady currents were applied to the fibers to obtain the desired level of depolarization. Changes in Ca^{2+} transients were correlated with concurrent depolarization-induced alterations in resting $[Ca^{2+}]$ and AP features. Changes in resting $[Ca^{2+}]$ routinely detected with OGB-5N were confirmed with Fluo-3.

Resting $[Ca^{2+}]$ at different membrane potentials

Here we found an intriguing effect of membrane depolarization on resting $[Ca^{2+}]$. Figure 3 show that stepwise membrane depolarization from −100 to −55 mV is associated with a graduated and reversible increase in resting $[Ca^{2+}]$. Analysis of OGB-5N data (Fig. 3A, B) show that at −55 mV free $[Ca^{2+}]$ is about threefold that assumed in quiescent polarized fibers (100 nM, see Methods), and that fiber repolarization to −100 mV results in the reversal of those effects (Fig. 3B). Similar results were obtained using Fluo-3 (Fig. 3D, E), but calculated $[Ca^{2+}]$ changes were larger than those calculated from OGB-5N data. Since in steady-state conditions both dyes are expected to report similar values of $[Ca^{2+}]$, the differences found probably reflect inadequacies of the dyes parameters. Panels C and F in Fig. 3 show pooled data obtained from fibers loaded with OGB-5N or Fluo-3, respectively.

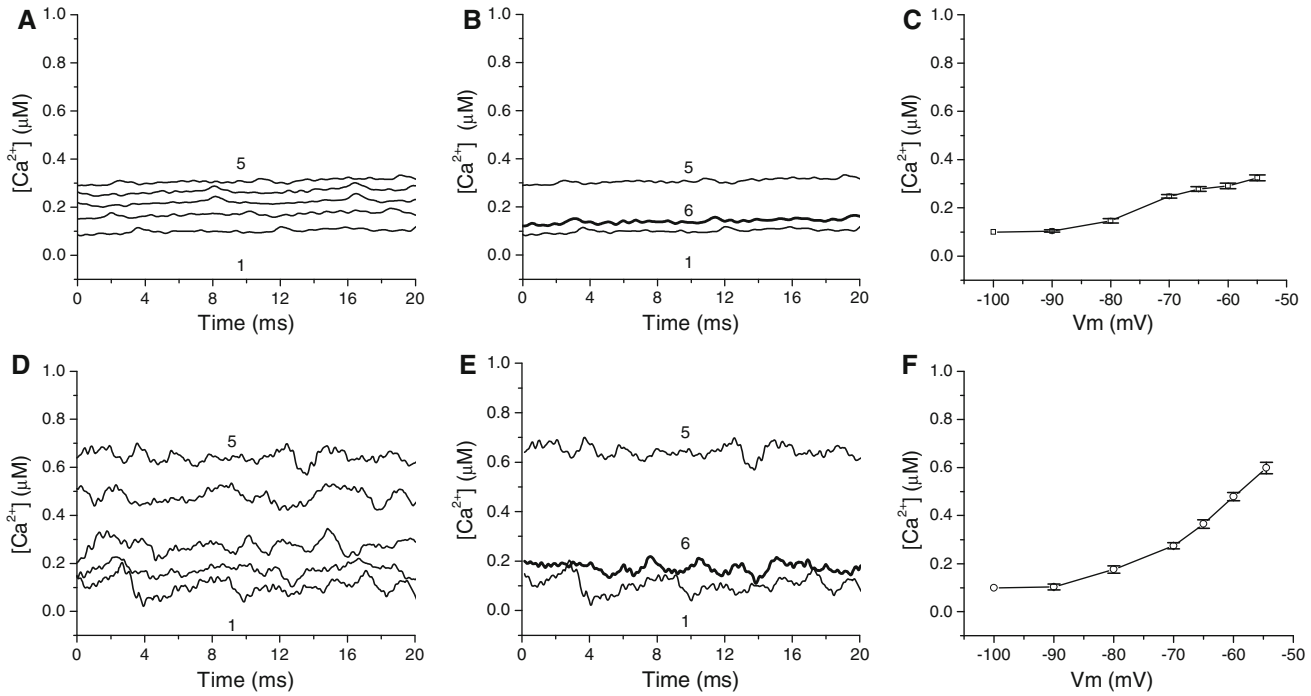

Fig. 3 Effect of holding potential on free resting [Ca^{2+}] calculated from OGB-5N (**A**–**C**) and Fluo-3 data (**D**–**F**). Traces 1–5 in **A**, **B** and **D**, **E** are the resting [Ca^{2+}] recorded at: −100 (control), −80, −70, −60 and −55 mV, respectively. Trace 6 is the resting [Ca^{2+}] recorded 3 min after repolarization to −100 mV. **C** and **F** are the average resting [Ca^{2+}] as a function of membrane potential from 8 to 6 fibers, respectively. [OGB-5N]: 200 μM. [Fluo-3]: 100 μM. Sarcomere length: 4.3 ± 0.2 μm and 4.1 ± 0.3 μm for **C** and **F**, respectively. Records were taken ~3 min after changing membrane potential

Effects of membrane potential on Ca^{2+} transients elicited by single stimulation

Opposite to the monotonic effect of depolarization on resting [Ca^{2+}], fiber depolarization from −100 to −55 had a complex effect on Ca^{2+} release. Depolarization from −100 to −90 mV had no significant effects on Ca^{2+} transients, but further depolarization up to −55 mV produced profound changes on the features of the Ca^{2+} transients (Fig. 4A and C, traces 2–4). It can be seen that, in this range of potentials, depolarization has a dual effect on the amplitude of Ca^{2+} transients. The amplitude increases with depolarization from −90 to −60 mV. Trace 3 in Fig. 4A shows the maximum potentiation of Ca^{2+} transient by depolarization; reached in this fiber at −60 mV. It can also be seen that the increase in the amplitude of the Ca^{2+} transient is larger than the increase in the pre-stimulus ("resting") [Ca^{2+}]. Ca^{2+} transients are markedly depressed by further depolarization between −60 and −55 mV (Fig. 4A, trace 4), and totally absent thereafter (not shown). Figure 4C shows that biphasic changes in transient amplitude are accompanied with a monotonic increase in both the transient duration and the time to peak of the Ca^{2+} transient. The increase in transient duration is due to a slowing of both its rising and falling phases. All the depolarization-dependent changes in the Ca^{2+} transient could be completely reversed by repolarizing the fiber to −100 mV as shown by the similarity of Ca^{2+} transients calculated from fluorescence data obtained before depolarizing the fibers (thin trace, Fig. 4D) and after repolarizing it back to −100 mV (thick trace, Fig. 4D). The maximal potentiation of the amplitude of the Ca^{2+} transient was 17.2 ± 7.3% ($n = 8$, $P < 0.05$). This value is significantly smaller than the maximal twitch amplitude potentiation (~56%) seen in amphibian fibers in the presence of 9 mM K_o^+ (Renaud and Light 1992), but similar to the potentiation found in mammalian fibers exposed to 10 mM K_o^+ (Cairns et al. 1997). The difference in percentage potentiation of both variables in frog fibers probably reflects the non linear dependence of force on free [Ca^{2+}]. The difference in force potentiation between amphibian and mammalian fibers is interesting and deserves further investigation.

Simultaneous electrical recordings (Fig. 4B) demonstrate that fiber depolarization results in a reduction of the AP amplitude and an increase of AP duration. AP overshoot is not affected significantly by depolarization up to −80 mV (traces 1–2). Further depolarization resulted in the reduction of the overshoot and increase of the duration of the AP (traces 3–4). Aside from the obvious reduction in

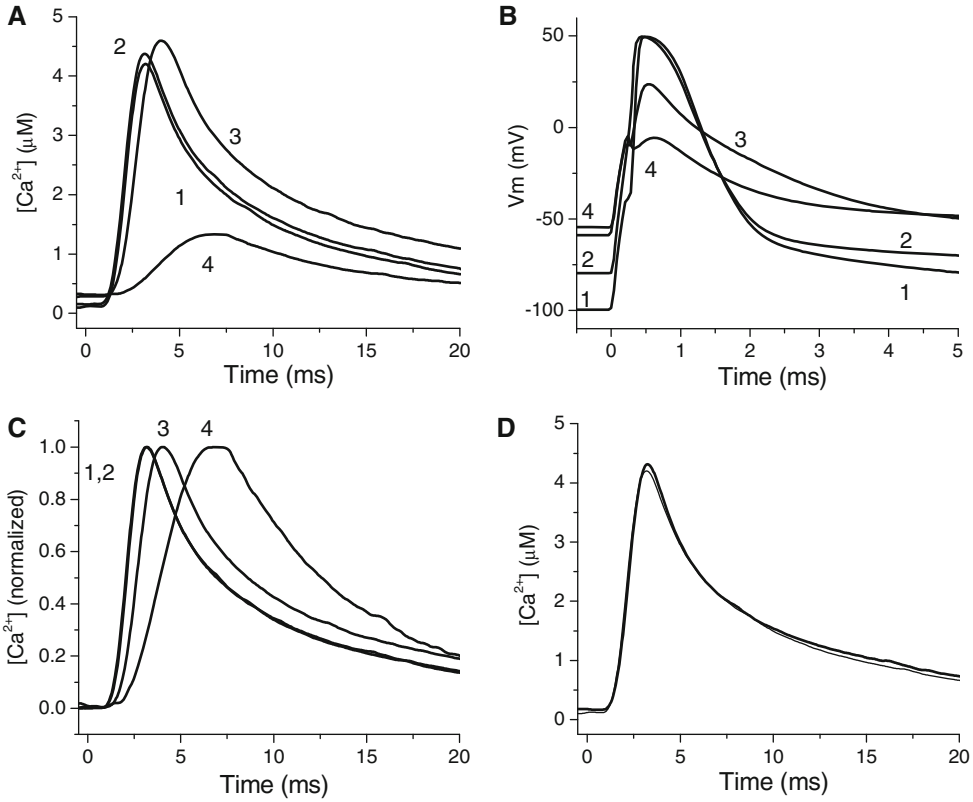

Fig. 4 Calcium transients elicited by single stimulation at different membrane potentials. **A** Traces 1–4 are Ca^{2+} transients calculated from OGB-5N fluorescence transients elicited at membrane potentials of −100, −80, −60 and −55 mV, respectively. **B** AP's corresponding to Ca^{2+} transients in **A**. Note differences in time scales. **C** Ca^{2+} transients in **A** presented in a normalized scale. **D** Calcium transients calculated from OGB-5N fluorescence transients elicited at −100 before applying the depolarizing protocol (*thin trace*) and 3 min after repolarizing the fiber (*thick trace*). Sarcomere length: 4.5 μm

amplitude due to the imposed depolarization, traces 1–2 shows that potentiation can occur in the absence of noticeable changes in overshoot and speed of depolarization and repolarization. It should be also noticed that the AP that elicited the largest Ca^{2+} transient (trace 3) displays an amplitude about 50% that of control (trace 1) and a FDHM that is more than twofold that of control. Altogether, these results suggest that AP amplitude and waveform are not the only factors determining the features of the Ca^{2+} transients. The repolarization phase of AP elicited at highly depolarized potentials follow a single exponential and resemble that observed in fatigued fibers but differ from that recorded from fibers exposed to high $[K^+]_o$ (Lannergren and Westerblad 1986).

The effects of membrane depolarization on some features of APs and Ca^{2+} transients are summarized in Fig. 5. The biphasic dependence of Ca^{2+} transient amplitude on membrane potential is clearly seen in Fig. 5A. It can be observed that the Ca^{2+} transient potentiation changes smoothly with depolarization between −90 and −65 mV, while a steep relationship between Ca^{2+} transient amplitude depression and membrane potential is seen in the range of −60 to −55 mV. The fact that the potentiation region of the plot is not correlated with the expected effects of changes in the overshoot (Fig. 5C) and FDHM of the AP (Fig. 5D), suggests that Ca^{2+} transient potentiation results from another voltage-dependent parameter, such as the resting $[Ca^{2+}]$. In fact, a significant potentiation is still seen at about −60 mV, while the AP amplitude and overshoot are highly depressed. Figure 5A is highly reminiscent of the effect of raising $[K^+]_o$ on twitch tension (Renaud and Light 1992). On the other hand, the depression region of the plot is correlated with a pronounced reduction in the overshoot and a large increased of the FDHM of the AP.

Effects of membrane potential on Ca^{2+} transients elicited by tetanic stimulation

To assess the effect of depolarization on Ca^{2+} release during repetitive activation in the absence of ionic concentration changes, fibers were depolarized at various levels by current injection and stimulated with 10 pulses applied at 100 Hz (Fig. 6). Except for the potentiation of the first transient of the train, depolarization from −100 to −80 mV had little effect on Ca^{2+} release along the train (Fig. 6A, B). In contrast, depolarization to −60 mV had differential effects on Ca^{2+} transients along the train. Maximal potentiation was seen in response to the first pulse of the train whereas depression of Ca^{2+} transients was observed from the second to the last stimulus (Fig. 6E, F). It can also be seen that the release is irregular along the train, i.e. transients of alternating amplitude can be detected along the train. Nevertheless, opposite to the case for the first transient, the amplitudes of the 2nd to 10th Ca^{2+}

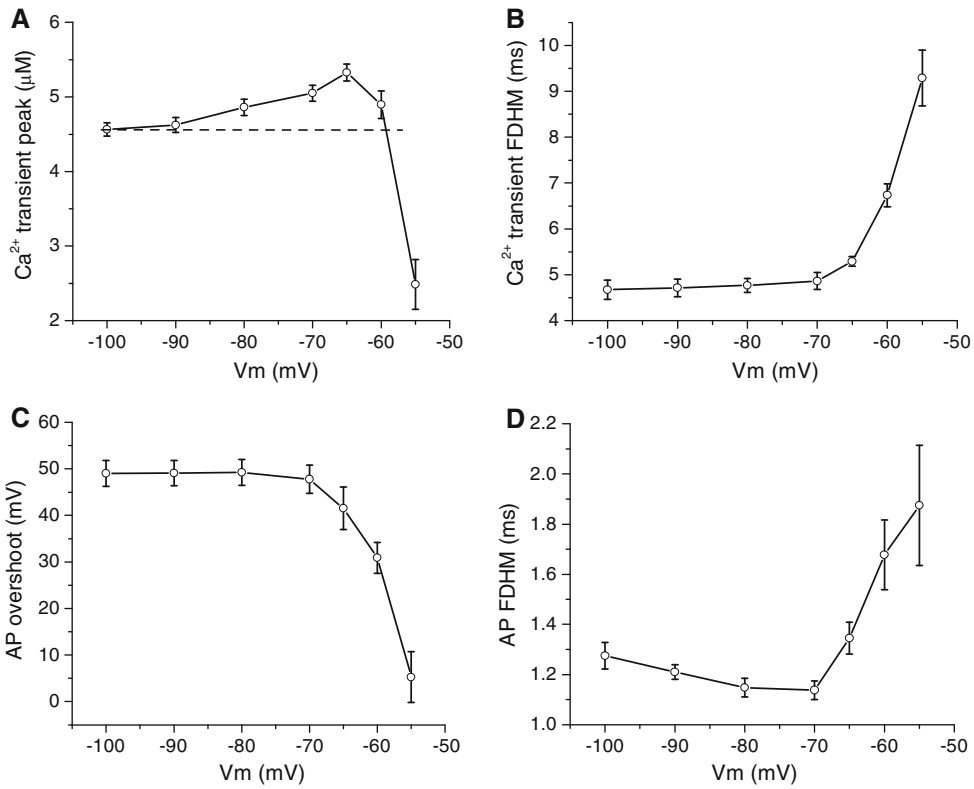

Fig. 5 Effects of membrane potential on AP and Ca^{2+} transients parameters. **A** Peak Ca^{2+} transient as a function of membrane potential. The *dashed line* represents the peak Ca^{2+} transient at −100 mV. **B** FDHM of Ca^{2+} transients recorded at various membrane potentials. **C** Depression of AP overshoot with membrane depolarization. **D** FDHM of AP's elicited from various membrane potentials. *Symbols* and *bars* represent the mean ± ES ($n = 5$)

transients at −60 mV were always smaller than those detected from −100 to −80 mV. At −55 mV, only a highly depressed Ca^{2+} transient elicited by the first stimulus is seen. Potentiation along the train (2nd to 10th pulses) was observed in a narrower potential range as compared with the responses to single pulses. An example of potentiation of the Ca^{2+} release from a fiber depolarized to −70 mV is shown in Fig. 8B. As can be seen, all Ca^{2+} transients along the train (in response to the 2nd to 10th pulses) were larger than those recorded at −100 to −80 mV. As expected, the effects of depolarization on the first pulse of the trains are identical to those observed in response to single stimulation. Figure 6E–H compare, in an expanded time scale, the first and last Ca^{2+} transient (if present) of every train. Figure 6G highlights the potentiation and prolongation of the first Ca^{2+} transient at −60 mV, as compared to those recorded at more negative membrane potentials. The electrical records corresponding to the Ca^{2+} transients shown in Fig. 6A–H are presented in Fig. 6I–P. Other than the imposed depolarization, little differences are detected among the AP trains elicited between −100 and −80 mV (Fig. 6I, J and M, N). Although active responses are elicited by all pulses in the train, only the first AP display a significant overshoot at a holding potential of −60 mV (∼20 mV, Fig. 6K, O). As seen with single stimulation, this smaller AP is associated with a potentiated Ca^{2+} transient, while the rest of APs along the train elicits depressed releases. It can also be seen that variability in the Ca^{2+} transient amplitude is associated with corresponding, but smaller, variations in AP amplitude. It is remarkable that a difference of ∼3 mV between the overshoots of the 9th and 10th AP is associated with relatively larger changes in Ca^{2+} transient amplitude (Fig. 6G, O). At −55 mV only the first pulse of the train elicits a regenerative active response; the rest of responses along the trains are abortive (Fig. 6L, P). The fact that at this potential the fiber cannot sustain active responses to 100 Hz stimulation explains why there is no Ca^{2+} release along the train but the depressed Ca^{2+} release associated with the first AP (Fig. 6D). Thus, although single small APs can be generated at −55 mV, at this potential the excitability is so compromised that active responses to trains of stimuli cannot be generated. It is important to note that the lack of electrical response at highly depolarized potentials occurs even when the applied pulses depolarize the surface membrane to about −5 mV (Fig. 6O, P). The pattern of responses described in Fig. 6 and Fig. 8B was confirmed in 5 fibers.

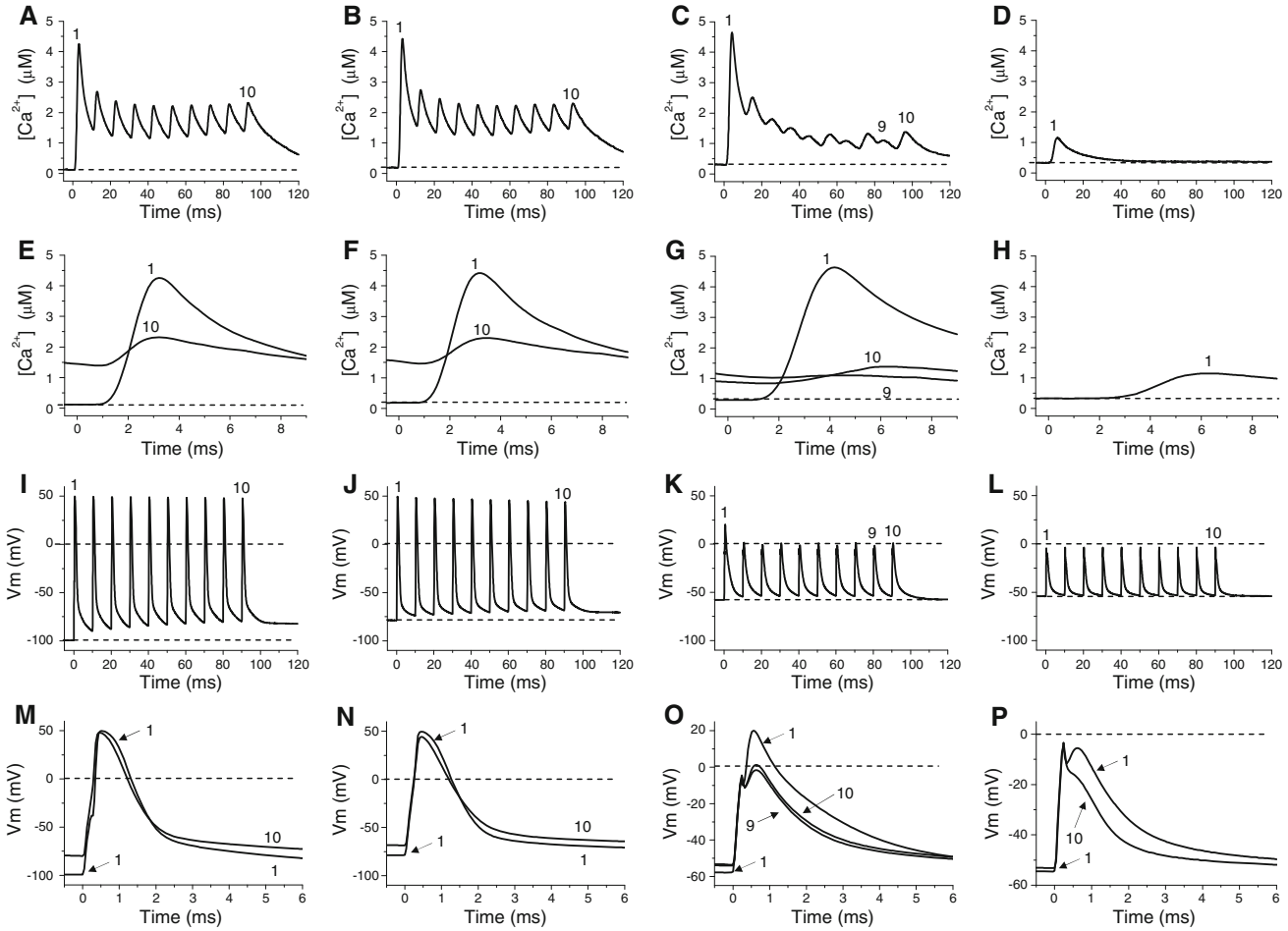

Fig. 6 Effects of membrane depolarization on Ca^{2+} transients elicited by repetitive stimulation. **A–D** Ca^{2+} transients elicited by 100 Hz stimulation in a fiber held at −100, −80, −60 and −55 mV, respectively. **E–H** First and last Ca^{2+} transients of **A–D** displayed in expanded time scales, respectively. The *dashed lines* in **A–H** indicate the resting $[Ca^{2+}]$. **I–L** Electrical records corresponding to the Ca^{2+} transients shown in **A–D**, respectively. **M–P** Expanded time presentation of AP's recorded simultaneously with the Ca^{2+} transients shown in **E–H**, respectively. Different voltage scales were used for **M–P**. The pulse amplitude was not changed. The *dashed lines* in **I–P** indicated the resting and zero potentials. The numbers in panels **A–P** indicate the position of responses along the train. Records were taken ~3 min after changing membrane potential

Effect of 10 mM extracellular $[K^+]$ on Ca^{2+} transients

The effects of potassium accumulation during fatigue were tested independently from other factors by measuring Ca^{2+} transients and AP's in rested fibers exposed to 10 and 15 mM $[K^+]_o$. We first studied the effect of raising the $[K^+]_o$ to 10 mM on the Ca^{2+} transients elicited by single stimulation (Fig. 7). Fibers depolarized to about −70 mV when exposed to 10 mM K_o^+. Ca^{2+} transients calculated from fluorescence transients recorded in 10 mM $[K^+]_o$ (Fig. 7A, trace 3) are potentiated and prolonged as compared to those obtained from data recorded in normal Ringer at −100 mV (trace 1). Also it can be seen that resting $[Ca^{2+}]$ is higher in high $[K^+]_o$ (trace 3) than in normal Ringer (trace 1). This result is in agreement with the relationship between resting $[Ca^{2+}]$ and the resting membrane potential described above. Since fibers exposed to 10 mM extracellular K^+ depolarizes to approximately −70 mV (Fig. 7B, trace 3), in Fig. 7A the Ca^{2+} transient obtained in a fibers maintained in normal Ringer but depolarized to −70 mV by current injection (trace 2) is included for comparison. It can be seen that both transients are very similar. The corresponding AP's (Fig. 6B, traces 2–3, respectively) are also comparable. The fact that K^+-induced depolarization has similar effects to those of depolarization induced by current injection is the first direct evidence suggesting that the effects of 10 mM K_o^+ on Ca^{2+} transients shown here and the effects on active force production shown elsewhere (Renaud and Light 1992; Bouclin et al. 1995; Cairns et al. 1997) are due to the depolarization of the membrane, and, more importantly, possibly mediated by a potentiation of Ca^{2+} release, i.e.,

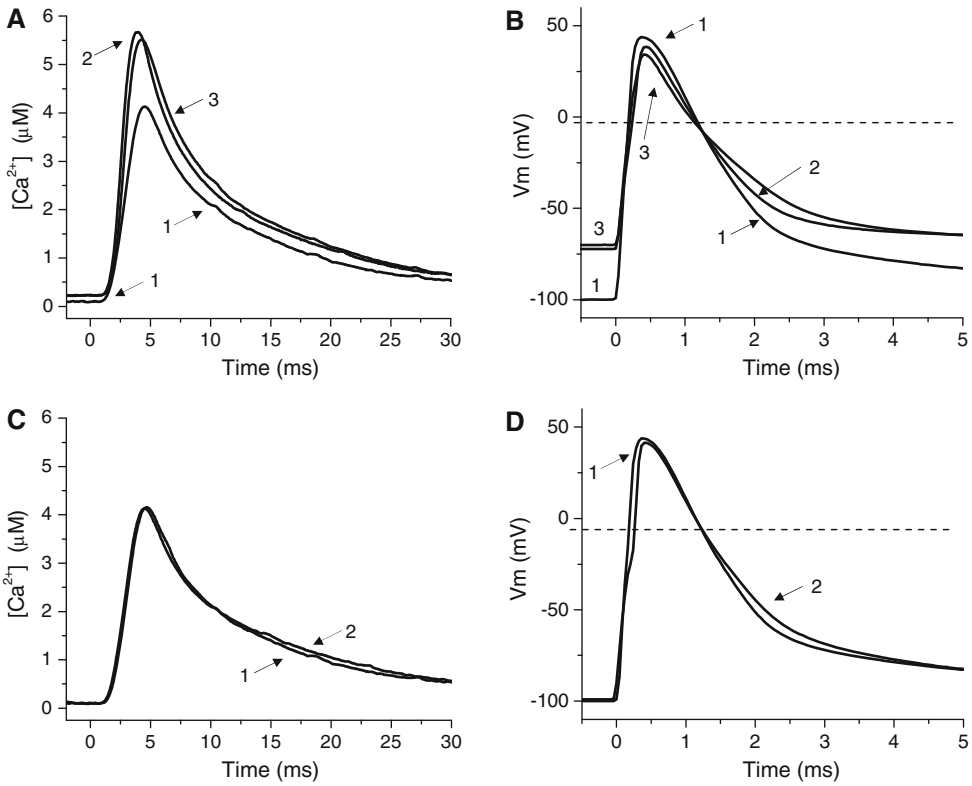

Fig. 7 Ca^{2+} transients elicited by single stimulation in a fiber exposed to 10 mM extracellular K^+. **A** Superimposed Ca^{2+} transients calculated from fluorescence transients recorded in control conditions (−100 mV, 2.5 mM K_o^+, trace 1), after depolarizing the fiber to −70 mV by current injection (2.5 mM K_o^+, trace 2), and after exposing the fiber to 10 mM K_o^+ (trace 3). **B** Traces 1–3 are the APs corresponding to data in **A**. **C** Ca^{2+} transients recorded at −100 mV in a fiber exposed to 2.5 mM K_o^+ (trace 1) and 10 mM K_o^+ (trace 2). **D** Traces 1–2 are the APs corresponding to data in panel **C**. The *dashed lines* in **B** and **D** indicate the zero potential. Sarcomere length: 4.3 μm. Records were taken about 20 min after changing solutions

they are not due to the presence of K^+ per se. Further evidence in support of this possibility is provided in Fig. 7C, which shows that the effects of 10 mM K_o^+ can be reversed by repolarizing the fiber by means of current injection. As can be seen the Ca^{2+} transient obtained at −100 mV in the presence of 10 mM K_o^+ is almost identical to that obtained in control conditions (−100 mV, 2.5 mM K_o^+, Fig. 7C, trace 2). Also, as shown above, the increased resting $[Ca^{2+}]$ in the presence of 10 mM $[K^+]_o$ is reversed by repolarization. Correspondingly, Fig. 7D shows that AP's eliciting the transients in Fig. 7C do not differ significantly, despite being recorded in the presence of different $[K^+]_o$. Results presented in Fig. 7 were obtained from a fiber that showed one of the largest depolarization-induced potentiation of Ca^{2+} release.

The effects of 10 mM K_o^+ on Ca^{2+} transients elicited by repetitive stimulation are shown in Fig. 8. Panels A–C show Ca^{2+} release from the same fiber in control conditions (−100 mV, 2.5 mM K_o^+), after depolarizing the fiber to −70 mV by current injection (2.5 mM K_o^+), and in the presence of 10 mM K_o^+, respectively. The potentiating effect of 10 mM K^+ on Ca^{2+} transient in response to single stimulation was observed in all the transients along the train (Fig. 8C). The potentiation was mimicked by depolarization to a similar resting membrane (Fig. 8B). The first, the second and last Ca^{2+} transients obtained in the three conditions are compared in Fig. 8D–F in an expanded time scale. In this figure, it can be better seen that equivalent Ca^{2+} transients in panels E and F are similar to each other, but larger and longer than equivalent transients recorded in control conditions (panel D).

The APs recorded simultaneously with the Ca^{2+} transients in Fig. 8A–C are shown in Fig. 8G–I. The trains of APs recorded at −70 mV in the presence of 2.5 or 10 mM K_o^+ are almost identical (Fig. 8H, I). In addition, the APs along the trains do not change significantly as evidenced by the enlarged records in Fig. 8J–L, which compare the first, the second and the last AP of the train. On the other hand, as shown in Fig. 8D–F, the amplitude and duration of Ca^{2+} transients change along the train. Data in Fig. 8H, I and B, C demonstrate that potentiated Ca^{2+} transients in fibers depolarized by either raising $[K^+]_o$ or by current injection are associated with smaller APs of similar FDHM. Ca^{2+} transients obtained from fibers polarized at −100 mV and exposed to 10 mM K_o^+ were similar to those in control conditions (not shown). As seen for single stimulation, the results above indicate that the effects of 10 mM K_o^+ on Ca^{2+} transients along the train are dependent on fiber depolarization. Thus, depolarization can be used to mimic the effect of raising the $[K^+]_o$ up to 10 mM. The potentiation of Ca^{2+} release produced by raising $[K^+]_o$ to 10 mM is in apparent contrast to the lack of effect of $[K^+]_o$ on tetanic force (Renaud and Light 1992; Cairns et al. 1997).

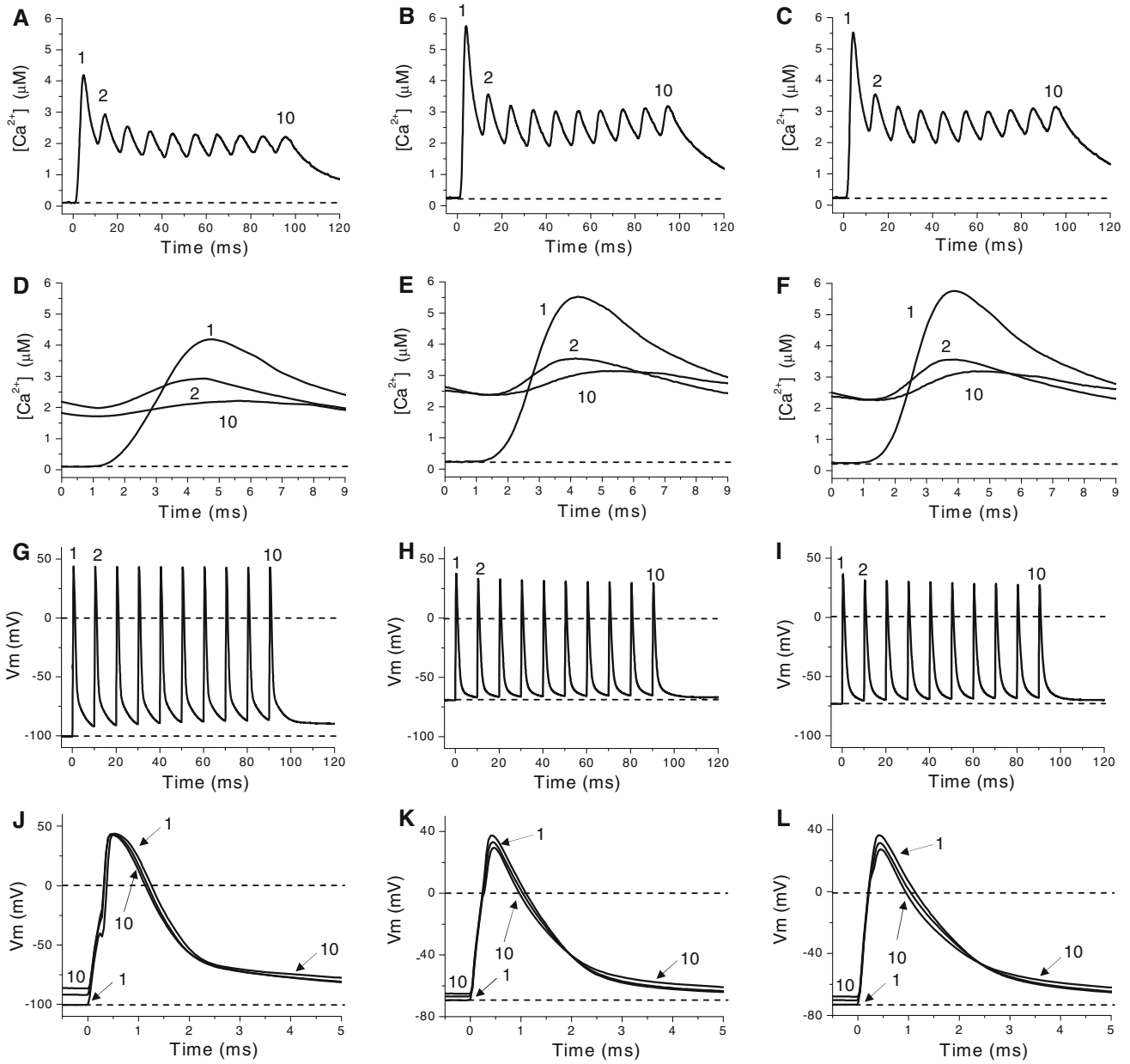

Fig. 8 Ca^{2+} transients in response to repetitive stimulation in a fiber exposed to 10 mM extracellular K^+. **A**, **B** Ca^{2+} transients obtained in the presence of 2.5 mM K_o^+ at −100 and −70 mV, respectively. **C** Ca^{2+} transients obtained in the presence of 10 mM K_o^+. **D–F** *Traces 1*, *2* and *10* represents the first, second and last Ca^{2+} transients in **A–C**, respectively. **G–I** AP trains eliciting the Ca^{2+} transients in panels **A–C**, respectively. **J–L** *Traces 1*, *2* and *10* are the APs triggering the Ca^{2+} transients in **D–F**, respectively. *APs* are shown in expanded time and voltage scales. *Dashed lines* in **A–F** indicated the resting $[Ca^{2+}]$. *Dashed lines* in **G–L** represent the resting and zero potential. Records were taken ~20 min after changing solutions

Ca^{2+} transients in the presence of 15 mM extracellular K^+

Since the $[K^+]$ in the *t*-tubule lumen can reach higher values than those measured in the plasma or tissue fluids (Juel 1986), we measured the Ca^{2+} release in fibers equilibrated in Ringer containing 15 mM K^+. Unexpectedly, fibers exposed to 15 mM K_o^+ depolarized to a similar membrane potential as fibers exposed to 10 mM K_o^+ (−68 ± 1.8 mV; $n = 4$). Figure 9 compares Ca^{2+} transients obtained in fibers exposed to 15 mM K_o^+ (panels C and F) with those obtained in the presence of 2.5 mM K_o^+ at −100 and −70 mV (panels A and D; and B and E; respectively). Depolarization of the fibers to a value similar to that observed in the presence of 15 mM K^+ resulted in potentiation of Ca^{2+} transients in response to single (not

shown) and repetitive stimulation at 100 Hz (Fig. 9B). Nevertheless, in contrast to what was observed using 10 mM K_o^+, regardless of its depolarizing effect, no potentiation was observed in the presence of 15 mM K_o^+. Instead, Ca^{2+} transients show a monotonic depression along the train, and the depression manifests from the first pulse. By the end of the train (Fig. 9F) the amplitude of Ca^{2+} transient is about 25% that at the beginning of the train. No alternating amplitudes are seen in this condition, in contrast to that observed in fibers depolarized to −60 mV. As expected, the depression effect of 15 mM $[K^+]_o$ on Ca^{2+} transients is also seen when fibers are

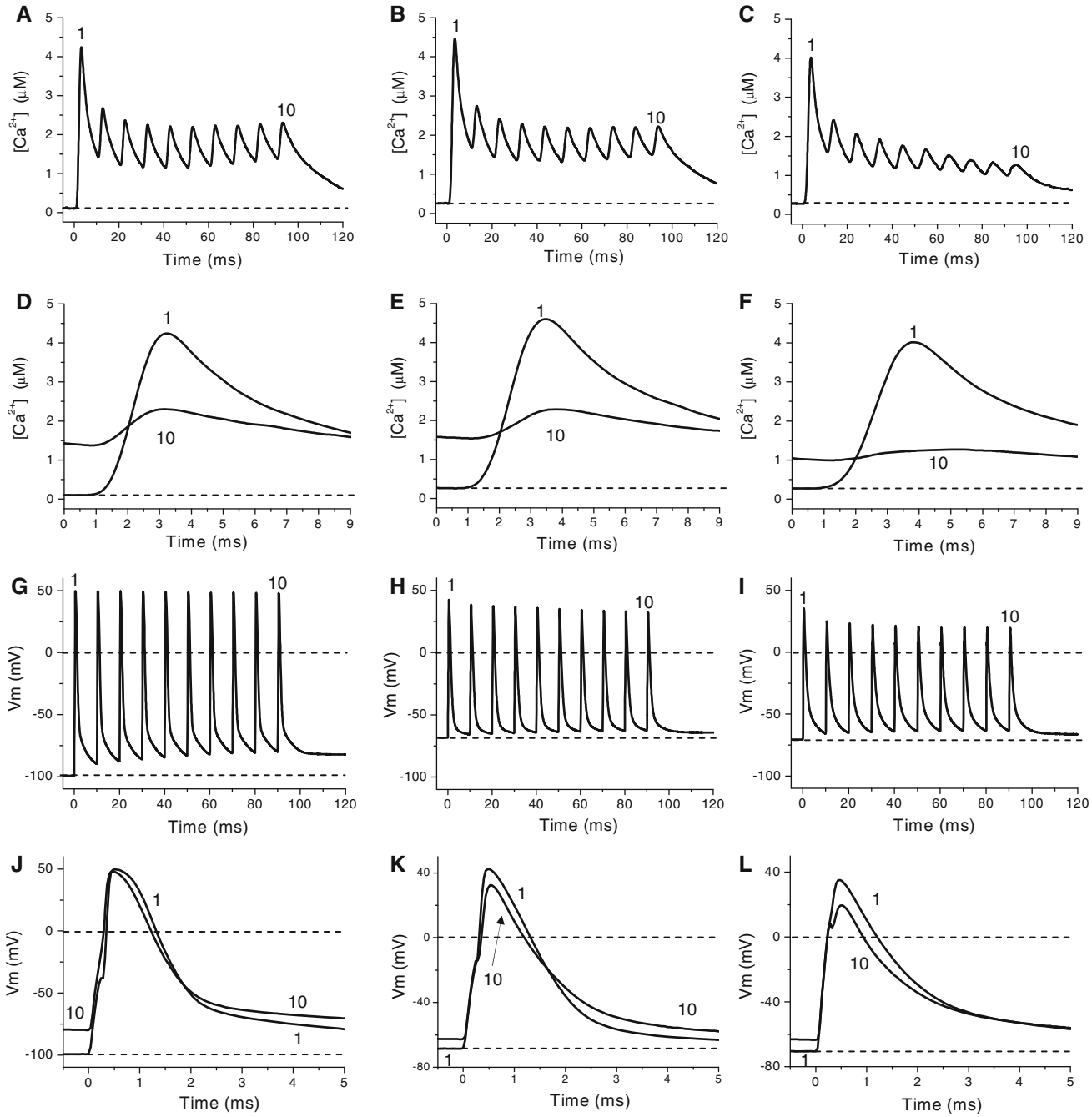

Fig. 9 Depression of Ca^{2+} transients in a fiber exposed to 15 mM K_o^+. **A**, **B** Trains of Ca^{2+} transients obtained in the presence of 2.5 mM extracellular K^+ in a fiber polarized to −100 (**A**) and −70 mV (**B**). **C** Ca^{2+} transients obtained in the same fiber 20 min after exposure to 15 mM extracellular K^+. **D**–**F** First (*1*) and last (*10*) Ca^{2+} transients of trains in **A**–**C**, respectively, shown in an expanded time scale. **G**–**I** Trains of APs eliciting the Ca^{2+} transients in **A**–**C**, respectively. **J**–**L** First (*1*) and last APs in **G**–**I** shown in an expanded time scale. *Dashed lines* in **A**–**F** indicate the resting $[Ca^{2+}]$. *Dashed lines* in **G**–**L** indicate resting and zero potential

stimulated by single pulses. With the caveat that *t*-tubules have reached a steady state potential in the presence of 15 mM K_o^+, the data above indicate that depression cannot result only from the depolarization per se, and suggest that potassium ions at this concentration might have another effect. The corresponding records of AP are shown in Fig. 9G–L. The amplitude of the APs in 15 mM K_o^+ is slightly smaller than those in 2.5 mM K_o^+ at −70 mV, and is relatively constant from the second to the last AP along the train. Thus the progressive depression of Ca^{2+} transients does not correlate with the constancy of the amplitude of the (surface membrane) APs. The FDHM of APs recorded in the presence of 2.5 mM and 15 mM K_o^+ are similar (Fig. 9K, L). The depression of Ca^{2+} transients elicited by both single and tetanic stimulation seen in fibers exposed to 15 mM K_o^+ is in agreement with the depression of both twitch an tetanic force produced by $[K^+]_o$ higher than 10 mM.

As seen in fibers exposed to 10 mM K_o^+ the resting $[Ca^{2+}]$ was raised in fibers exposed to 15 mM K_o^+ (Fig. 9C, F).

To further explore the mechanism underlying the depression of Ca^{2+} transients by 15 mM K_o^+, fibers exposed to this K_o^+ concentration were repolarized by current injection. Figure 10 show Ca^{2+} transients elicited by 10 pulses at 100 Hz in a fiber exposed initially to Ringer (Fig. 10A), then exposed to 15 mM K_o^+ and repolarized to −100 mV (Fig. 10B, E), and finally re-exposed to Ringer. Fiber repolarization reversed most changes in AP features (Fig. 10H, K), as can be seen by comparing data in Fig. 9I, L (obtained from a fiber exposed to 15 mM K_o^+) and Fig. 10G and J (obtained in control conditions, 2.5 mM K_o^+, −100 mV). Nevertheless, the amplitude of the Ca^{2+} transients was not recovered after fiber repolarization (Fig. 10B and E). To discard any deleterious effect during the experimental manipulations, high potassium Ringer was exchanged with normal Ringer. Under this condition, Ca^{2+} transients recovered its features in control conditions (Fig. 10C, F). In the same way, the normal electrical activity was recovered after returning to control conditions (2.5 mM K, −100 mV). These last results demonstrate that changes elicited by 15 mM K_o^+ are fully reversible. Similar results were obtained in 4 fibers.

Discussion

A number of factors have been implicated in the generation of muscle fatigue in response to continuous high frequency stimulation and interactions among them have been demonstrated (for reviews see (Westerblad et al. 1991; Fitts 1996; Fitts and Balog 1996). The relative impact of changes in the mechanisms underlying fatigue development is expected to vary depending on the muscle type and the pattern of activation (Allen, Lamb et al. 2008). In addition, there are evidences suggesting that the effects of some factors as measured *ex vivo* can be less important in vivo (for a detailed discussion see Allen et al. 2008).

Here we have conducted an *ex vivo* study of the effects of fiber depolarization and raised $[K^+]_o$ on the Ca^{2+} release of fast skeletal muscle fibers elicited by single stimulation and short high frequency trains of pulses. The aim of this study was to test the K^+ hypothesis for muscle fatigue (Renaud and Light 1992; Cairns, Buller et al. 2003). Our work extends previous *ex vivo* studies of the effects of raising $[K^+]_o$ on active force generation and provide new insights on the possible mechanisms linking the extracellular K^+ accumulation to changes in Ca^{2+} release and electrical excitability.

To test the possibility that the effects of extracellular K^+ accumulation on force generation are mediated by membrane depolarization (Renaud and Light 1992; Cairns et al. 2003), we independently studied the effects of rising $[K^+]_o$ and depolarizing the membrane (at constant $[K^+]_o$) on the Ca^{2+} release of rested fibers and correlated those effects with changes in AP generation. It is expected that changes in force output during fatiguing stimulation should reflect, at least in part, changes in Ca^{2+} release resulting from fiber depolarization. As opposed to the case of intact muscles, with this approach we could directly assess whether membrane depolarization at constant $[K^+]_o$ can reproduce the effects of changing $[K^+]_o$, and whether the effects of raised $[K^+]_o$ could be reversed by hyperpolarization.

Cut fibers loaded with low affinity Ca^{2+} dyes as a model to study muscle fatigue

Our results demonstrate that stretched cut muscles fibers mounted in an inverted two Vaseline gap chamber (DiFranco et al. 1999; Quinonez and DiFranco 2000) can be successfully used as an alternative model to study some aspects of muscle fatigue which are not amenable to the intact fiber model. The advantages and shortcomings of several approaches used to study muscle fatigue (but not cut muscle fibers) have been recently reviewed (Allen et al. 2008). Our method allows for the control of membrane potential and the simultaneous recording of AP's and Ca^{2+} transients in response to single or repetitive stimulation. Although in this study fiber stimulation was restricted to short trains, continuous or intermittent trains of stimuli lasting for minutes can be used (data not shown, Quinonez and DiFranco 2000). Since a low [EGTA] was used, stretching the fiber segment in the central pool of the experimental chamber to sarcomere lengths above 4 μm was found essential to prevent artifacts in fluorescence transients due to fiber shortening elicited by tetanic stimulation. It should be noted that, the complete impediment

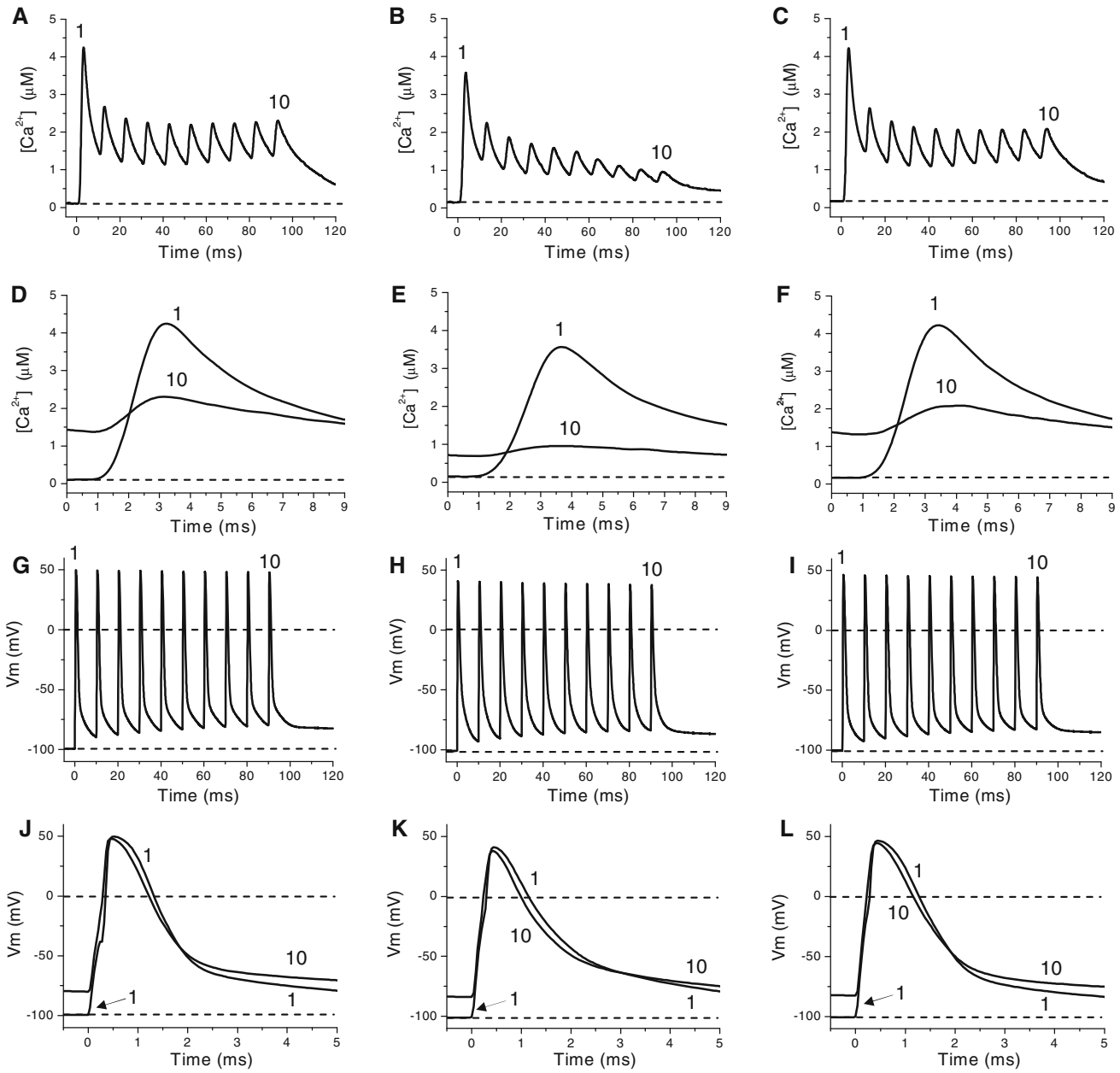

Fig. 10 Effects of 15 mM K^+ on Ca^{2+} transients cannot be reversed by repolarization. **A–C** Ca^{2+} transients elicited by trains of AP's in the same fiber maintained in control conditions (−100 mV, 2.5 mM K^+, **A**); after exposure to 15 mM K+ and subsequent repolarization to −100 mV (**B**); and after returning to control conditions (**C**). **D–F** First (*1*) and last (*2*) Ca^{2+} transients in **A–C**, respectively, presented in an expanded time scale. **G–I** Trains of AP's generating the Ca^{2+} transients in **A–C**, respectively. **J–L** First (*1*) and last (*2*) AP's of the trains shown in **G–I**. *Dashed lines* in **A–F** indicate the resting [Ca^{2+}]. *Dashed lines* in **G–L** indicate the resting and zero potential

of the formation of acto-myosin complexes should reduce the formation of inorganic phosphate (Pi), a factor known to reduce Ca^{2+} release probably by precipitating Ca^{2+} inside the sarcoplasmic reticulum (Allen et al. 2008).

Another advantage of our preparation is that the conduction of surface APs is prevented; i.e. supra-threshold current pulses are expected to elicit membrane action potentials at the surface membrane, while almost simultaneously APs are elicited at the outermost regions of the *t*-tubules. As a consequence, changes in Ca^{2+} transients should result mostly from changes in *t*-tubule APs. Similarly, conduction of surface APs is also prevented when stimuli are applied through long electrodes placed parallel to fibers or muscles (Cairns et al. 2007, 2009). As pointed

out by these authors, in the absence of surface AP conduction, reductions of force generation mostly reflects impairments of the *t*-tubule APs (Cairns et al. 2007, 2009).

By comparing fluorescence transients and Ca^{2+} transients calculated from fluorescence transients recorded from mechanically restrained fibers loaded with Rhod-2, Fluo-3 and OGB-5N we also demonstrate the limitations of high affinity dyes (i.e. Rhod-2 used here, and Fura-2, Indo-1 used elsewhere (Westerblad and Allen 1993)) and the superiority of low high affinity dyes (i.e. OGB-5N) to study Ca^{2+} release in skeletal muscle fibers (Baylor and Hollingworth 2003). The fact that OGB-5N fluorescence transients are kinetically similar to the underlying Ca^{2+} transients suggests that the reaction between Ca^{2+} and OGB-5N is close to equilibrium at any time during Ca^{2+} release. Thus, OGB-5N transients can be used to track Ca^{2+} release with high fidelity. On the other hand, the kinetics limitations for Rhod-2 and Fluo-3 shown here are expected to be exacerbated for dyes with smaller K_d such as Fura-2 and Indo-1. As can be seen from most published data, these dyes fail to faithfully track $[Ca^{2+}]$ changes in response to every pulse during a high frequency train, and report very small peak $[Ca^{2+}]$ changes (Westerblad and Allen 1993; Baylor and Hollingworth 2003), regardless of the fact that these dyes are ratiometric.

Effect of membrane potential on resting $[Ca^{2+}]$

Membrane depolarization has been suggested as a main factor leading to muscle fatigue. We found that membrane depolarization affects both the resting $[Ca^{2+}]$ and the AP elicited Ca^{2+} transients. Our results extend previous works showing that membrane depolarization leads to a raised resting $[Ca^{2+}]$ (Lopez et al. 1983; Snowdowne 1985; Lee et al. 1991). Using three calcium dyes of different K_d's we found that myoplasmic resting $[Ca^{2+}]$ increases monotonically in response to membrane depolarization in the range of −100 to −55 mV. This effect was observed not only in fibers depolarized by current injection but in fibers exposed to raised $[K^+]_o$. The fact that the depolarization-dependent increase in resting $[Ca^{2+}]$ was independent of the Ca^{2+} dye used and could be reversed by repolarization to −100 mV regardless of the method used to depolarized the fibers demonstrates a genuine dependence of resting $[Ca^{2+}]$ on membrane potential. In addition, previous results from intact fibers discard the possibility that the phenomenon observed here depended on the experimental model used (i.e. intact vs. cut fibers). Nevertheless, different $[Ca^{2+}]$ ($[Ca^{2+}]_t$ in Eq. 1) were calculated from Fluo-3 and OGB-5N fluorescence data (Fig. 3C, F). This result may indicate that the parameters assumed for each dye in Eq. 1 does not faithfully reflect the behavior of the dyes in the myoplasm. On the other hand, although the actual $[Ca^{2+}]$ calculated with Eq. 1 will depend on the value assumed for $[Ca^{2+}]_{rest}$, changes in this parameter are not expected to explain the differences in $[Ca^{2+}]$ calculated from Fluo-3 and OGB-5N fluorescence data.

The mechanism underlying the voltage-dependent increase of resting $[Ca^{2+}]$ does not seem to inactivate since the changes were stable over periods of minutes. It may be speculated that the increase in resting $[Ca^{2+}]$ between −80 and −55 mV may result from the asynchronous activation of sarcoplasmic reticulum (SR) release units since depolarizations in this range are too low to activate sarcolemmal L-type Ca^{2+} channels. In partial support to this possibility, it has been shown that spontaneous Ca^{2+} release in frog fibers increases with depolarization between −65 and −60 mV (Hollingworth, Soeller et al. 2000).

The rise in resting $[Ca^{2+}]$ in response to steady depolarization is expected to impact AP elicited Ca^{2+} transients and thus force generation. Interestingly, a raised resting $[Ca^{2+}]$ has been suggested as one of the possible mechanisms underlying the potentiation of submaximal contractures at elevated $[K^+]_o$ (Snowdowne 1985; Cairns et al. 1997). Although raised resting $[Ca^{2+}]$ will augment the occupancy of Ca^{2+} binding sites of the main myoplasmic Ca^{2+} binding proteins (e.g. troponin, parvalbumin, calmodulin, SERCA-1), thus contributing to the increased amplitude of Ca^{2+} transients; regulatory effects of increased Ca^{2+} can also be expected. The effects of depolarization on the resting $[Ca^{2+}]$ may be of relevance to unveil mechanisms linking changes of $[K^+]_o$ and force generation.

Membrane depolarization has a dual effect on Ca^{2+} transients elicited by single stimulation

Among other changes, continuous stimulation of fibers at high frequency leads to depression of force generation and fiber depolarization (Lannergren and Westerblad 1986; Allen et al. 2008). According to the K^+ hypothesis, these changes are mediated by extracellular K^+ accumulation resulting from continuous electrical activity. Nevertheless, in rested fibers, raising $[K^+]_o$ produces differential effects on twitch and tetanic force (Renaud and Light 1992; Bouclin et al. 1995). Changes in $[K^+]_o$ to about 10 mM potentiates twitch force but is with no effect on tetanic force. Changes above 10 mM result in depression of both twitch and tetanic force.

Although it has been demonstrated that in vivo muscles lose K^+ during continuous electrical activation and the potassium efflux results in large increases of $[K^+]$ in the interstitium and the blood concurrently with a reduction of the $[K^+]_i$ (for reviews see Allen et al. 2008; Kristensen and Juel 2009), some mechanisms have been identified which can act in vivo to reduce the effects of the potassium efflux

(Allen et al. 2008). Nevertheless, the possible role of changes in the K^+ trans-transmembrane gradient on the generation of muscle fatigue in vivo has not been rule out, but is still a matter of active debate (see for example: Clausen and Nielsen 2008; Place 2008).

Here we describe for the first time that controlled membrane depolarization by current injection has a dual effect on Ca^{2+} transients elicited by single stimulation. Depolarization between −100 and −80 mV results in no significant effects on Ca^{2+} transients. Depolarization up to −60 mV potentiates Ca^{2+} release, while further depolarization has a pronounced depression effect on Ca^{2+} release. This effect contrasts with the monotonic dependence of resting $[Ca^{2+}]$ on membrane depolarization. Remarkably, the potentiation effect is also seen along 100 Hz trains. To our knowledge, our results represent the first direct evidence that membrane depolarization in the absence of ionic concentration changes potentiates Ca^{2+} transients and suggest that, among other mechanisms, it may result at least partially from an increase in Ca^{2+} release. In addition, our results demonstrate that depolarization per se does not necessarily should impair force generation. Between certain ranges of potentials depolarization may have a protective effect increasing in this way the safety factor between AP and force generation.

The potentiation of Ca^{2+} release by depolarization mimics and, more importantly, can explain the mechanical potentiation resulting from raising $[K^+]_o$ to 10 mM (Holmberg and Waldeck 1980; Renaud and Light 1992; Cairns et al. 1997). Although this possibility was previously suggested (Renaud and Light 1992) it had not been directly demonstrated previously.

Calcium release potentiation is accompanied by an increase of the resting $[Ca^{2+}]$ as already described. As discussed above, the increase in resting $[Ca^{2+}]$ is expected to increase the occupancy of the binding sites of the main myoplasmic buffers, nevertheless, the increase in Ca^{2+} transient amplitude is always much larger than the increase in resting $[Ca^{2+}]$. This suggests that potentiation may not be just a linear effect of raising $[Ca^{2+}]$, but to involve a regulatory mechanism of the Ca^{2+} release itself. The fact that potentiation is not associated with significant changes in AP properties also gives support to this contention. In this regard, as shown in Fig. 5D, the FDHM of the AP between −100 and −70 is smaller than at −100, thus ruling out that potentiation is due to prolongation of the AP. Since Ca^{2+} is known to modulate the Ca^{2+} release channels via a Ca^{2+}-induced Ca^{2+} release mechanism, a possible link between depolarization and Ca^{2+} release potentiation may be the increase in the concentration of resting free Ca^{2+} itself.

The steep depression effect of membrane depolarization on the amplitude of the Ca^{2+} transients seems to be correlated to the significant reduction of the overshoot of the surface membrane APs (i.e. ~25 mV) observed at membrane potentials between −60 and −55 mV. Assuming that the APs propagating along the *t*-tubules are similar to those originating at the surface membrane, a reduced Ca^{2+} transient is expected. The above assumption seems reasonable since at steady-state the potential of *t*-tubule membranes should reach the same value as that of the surface membrane and, to our knowledge, there is no evidence that the inactivation process of sodium channels present at the *t*-tubules and surface membranes is differentially affected by depolarization. Nevertheless, as suggested by data in Fig. 5D the effects of overshoot reduction may be partially counteracted by the increase in the FDHM of the APs found at this membrane potential range.

In addition, the depression of Ca^{2+} release between −60 and −55 mV might result in part from the steady-state voltage-dependent inactivation of the voltage sensor of the ECC mechanism. The main components of charge movement associated with the activation of the ECC voltage sensor, namely Q_β and Q_γ, has been shown to inactivate with depolarization. Nevertheless, it should be noted that the inactivation of Q_β display a relatively weak dependence on the holding membrane potential as to explain our data. On the other hand, while Q_γ displays a steep voltage dependent inactivation between −60 and −50 mV, which is compatible with our data; there is evidence suggesting that Q_γ is not the trigger but the result of Ca^{2+} release (Huang 1981, 1994; Rios et al. 1992; Prosser et al. 2009a, b). Moreover, the fact that a fraction of Q_γ inactivates between −70 and −60 mV (Huang 1994) is difficult to reconcile with our data showing a peak potentiation of Ca^{2+} transients at −65 mV (Fig. 5A). Furthermore, the finding that normal K^+ contractures can be obtained in fibers fatigued by continuous high frequency stimulation, and seemingly failing to generate normal APs (Cairns and Dulhunty 1995) suggests that charge movement inactivation does not play an important role in the observed depression of tension generation.

To our knowledge, the effect of membrane potential (either using conditioning pulses or changing the holding potentials) on Ca^{2+} transients elicited by AP stimulation has not been studied before, nevertheless, the voltage dependence of the inactivation of the force generation mechanism has been studied in voltage clamped fibers (Caputo et al. 1979; Neuhaus et al. 1990) and in fibers exposed to different $[K^+]_o$ (Frankenhaeuser and Lannergren 1967). Little inactivation of peak tension was found for conditioning depolarization between −100 and −50 mV, whereas a pronounced inactivation was found for larger depolarization (Frankenhaeuser and Lannergren 1967; Neuhaus et al. 1990). These results seem to rule out the possibility that the steep reduction of the Ca^{2+} transient

produced by depolarization between −60 and −55 mV found by us resulted from the same mechanism underlying the voltage-dependent inactivation of the force generation found at more positive membrane potential. Moreover, in contrast to our data, no potentiation effect was detected in the above studies.

Effects of depolarization-dependent changes in AP features on Ca^{2+} release

Changes in the features of AP (amplitude, overshoot, duration and mechanically active time) and the conduction of APs along *t*-tubules are also expected to affect Ca^{2+} release. Unexpectedly, for membrane potentials between −100 and −65 mV, Ca^{2+} transients are potentiated while both the AP amplitude and overshoot are highly reduced. The maximum Ca^{2+} transient potentiation is observed at about −65 mV, while at this potential the overshoot of the APs is reduced by ∼15%. Potentiation is still observed when the fibers are depolarized by ∼40 mV and the overshoot is reduced by >50%. This finding demonstrates a large safety factor between AP amplitude and Ca^{2+} release.

Ca^{2+} release potentiation cannot be explained by changes in AP duration, as described for type-B mechanical potentiators. In fact, both the duration and the mechanically active time decrease with depolarization from −100 to −70 mV, while the overshoot remains unaltered. For depolarization beyond −70 mV, the FWHM increases. In this range of potentials, the prolongation of the AP might compensate partially the effects of the reduction of the AP overshoot. Nevertheless, while AP prolongation is associated with muscle fatigue; it has been shown that the increase of AP duration by itself does not produce twitch potentiation in rested fibers (Yensen, Matar et al. 2002).

The depolarization-dependent potentiation of Ca^{2+} release and its relative independence of the AP amplitude and overshoot assure that muscle contraction can be sustained despite the depolarization and alterations of the AP resulting from high frequency stimulation.

Effects of depolarization on Ca^{2+} release in response to repetitive stimulation

As expected, the effects of depolarization on the Ca^{2+} release elicited by the first pulse of a train are identical to those elicited by a single pulse, yet depolarization has complex effects on the Ca^{2+} release along the trains. Potentiation was observed in a narrower range of potentials than that for single stimulation. Depression along the train is observed at a membrane potential more negative than that for single stimulation, and is associated with AP impairment. We showed that the amplitude of the Ca^{2+} transients elicited by the first pulse of 100 Hz trains applied at −60 mV are potentiated (Fig. 6C, G), in agreement with results obtained using single stimulation. Nevertheless, a reduction in the amplitude of Ca^{2+} transients elicited by the 2nd to 10th pulses of 100 Hz trains was found. The impairment in Ca^{2+} transients after the first pulse can be explained by the large reduction in the amplitude and duration of the APs in response to the 2nd to 10th pulses, as shown by the recordings in Fig. 6K and O. Several factors may contribute to the marked depression of AP amplitude from the 2nd to 10th pulses: a-reduced steady state availability of sodium channels, resulting from fast and slow inactivation mechanisms; b-partial recovery from fast inactivation during the inter-pulse interval, c-increased shunting conductances (e.g. chloride conductance) at depolarized potentials. The implication of this explanation, based on direct measurements of changes in $[Ca^{2+}]$ and APs, is in agreement with recent mechanical data obtained from mammalian skinned fibers stimulated with a two pulse protocol (Dutka and Lamb 2007). From force measurements, it was inferred that chronic depolarization (to an estimated value of −63 mV) impairs the repriming of the AP along a train of stimulation. Nevertheless, it is worth noting that in this study depolarization induced by raising the "intracellular" $[K^+]$ resulted in depression, not potentiation, of tension elicited by electrical single stimulation. This last result is at odds with our data and with previous mechanical data from intact fibers, showing potentiation of the Ca^{2+} transients and twitch tension, respectively (Renaud and Light 1992; Cairns et al. 1997). This apparent disagreement may result in part from the use of very different preparations.

Although the steady state dependence of charge movement on membrane potential do not seem to readily explain the dual effects of membrane depolarization on the amplitude of Ca^{2+} transients in response to single stimulation, a reduction of charge availability along high frequency trains may contribute to the reduction of Ca^{2+} transients observed from the second pulse of a train. It is possible that due to the short inter pulse interval some inactivation of the voltage sensor for the ECC mechanism accumulates along trains. This problem deserves more investigation, and can be addressed using cut fibers under voltage clamp conditions.

It should be noted that, although failures of AP along a train are associated with failures in Ca^{2+} release, in some cases APs with features similar to those elicited by single stimulation evoke depressed Ca^{2+} release as compared with single stimulation.

Since ECC occurs at the triads, some concerns have been raised relating to the relevance of changes in surface membrane APs for the generation of muscle fatigue (Allen

et al. 2008). Although our membrane potential recordings reflect mainly changes at the surface membrane, it is difficult to conceive how steady conditions leading to the generation of impaired AP at the surface membrane would, at the same time, allow for the generation of less altered or normal APs at the *t*-tubular membrane. On the contrary, it is expected that steady membrane depolarization (or raised $[K^+]_o$) impairing APs at the surface membrane, would at least affects similarly the *t*-tubular APs. In other words, our electrical records represent the best case scenario for *t*-tubular AP impairment by steady depolarization or increased $[K^+]_o$. In this regards, it has been shown in vivo that a reduced compound (surface) muscle AP is associated with fatigue (Bigland-Ritchie et al. 1979). Also, in *ex vivo* experiments demonstrating relatively small changes in surface membrane APs, larger changes in the *t*-tubule APs has been postulated to explain muscle fatigue (Balog et al. 1994).

Recent data obtained from whole muscles stimulated through either transverse or parallel electrodes demonstrate that when conduction of APs at the surface membrane is prevented (i.e. using parallel electrodes) changes in force generation are more directly related to changes in *t*-tubules APs (Cairns et al. 2007; Cairns et al. 2009). Since the stimulating conditions in our method is similar to that prevailing when using parallel electrodes, it is expected that the depression of Ca^{2+} transients found by us reflect mostly changes in *t*-tubules APs, not surface APs.

Overall, our results suggest a possible failure of *t*-tubule conduction. In the absence of surface membrane AP conduction, it can be envisioned that depressed Ca^{2+} transients recorded at depolarized potentials resulted mostly from the synchronized activation of peripheral triads rather than from random activation of *t*-tubules along the segment of fibers in the experimental pool. This possibility is in agreement with previous data showing that during fatiguing stimulation there is a radial gradient of myofibril activation, as well as a radial gradient of intracellular $[Ca^{2+}]$ (Bezanilla et al. 1972; Westerblad et al. 1990). A combined use of confocal methods to measure localized Ca^{2+} release and potentiometric dyes to assess *t*-tubule conduction should give more insight on the mechanisms underlying Ca^{2+} release potentiation and impairment produced by membrane depolarization (Quinonez and DiFranco 2000; DiFranco et al. 2002; DiFranco et al. 2005).

The data on Ca^{2+} transients recorded at different membrane potentials in response to repetitive stimulation cannot be readily compared with the effect of raised $[K^+]_o$ on tetanic force. Nevertheless, tetanic force data show small or no change between 2.5 and 9 mM (at pH = 7.2; Renaud and Light 1992), while the depression of tetanic force seen at higher $[K^+]_o$ correlates with the depression of Ca^{2+} release found here for larger depolarizations.

$[K^+]_o$ and Ca^{2+} transients

The opposite changes in $[K^+]_i$ and $[K^+]_o$ resulting from K^+ fluxes during continuous activation are expected to result in membrane depolarization, which has been proposed to contribute to the generation of muscle fatigue. Nevertheless, contrary to expectations, exposing rested fibers to 10 mM K^+ resulted in twitch potentiation, while no effect on tetanic force was detected. The mechanisms underlying this phenomenon are not known. Our work demonstrates for the first time that AP elicited Ca^{2+} transients are potentiated when $[K^+]_o$ is raised from 2.5 to 10 mM; and that this effect can be mimicked by membrane depolarization to a value similar to that observed in the presence of the raised $[K^+]_o$. More importantly we also demonstrated that the effects of 10 mM $[K^+]_o$ on Ca^{2+} transients and APs can be reversed by membrane hyperpolarization. The relationship between the amplitude of Ca^{2+} transients in response to single stimulations and the dependence of twitch force on $[K^+]_o$ are remarkably similar. In conjunction these results strongly suggest that the twitch force potentiating effect of 10 mM $[K^+]_o$ can be explained by the depolarization-dependent changes in Ca^{2+} release.

The effects of 15 mM $[K^+]_o$ are intriguing. On the first hand, it is unclear why the depolarization found in fibers exposed to 15 mM K^+ is less than expected. One possible explanation may rely on the use of constant $[Cl^-]_o$ and cut fibers. In cut fibers, KCl movement expected when $[K^+]_o$ is increased at constant $[Cl^-]_o$ may be compensated by KCl movements from the cut ends of the fibers, thus limiting membrane potential changes. The large chloride conductance present in the *t*-tubules of muscle fibers (Coonan and Lamb 1998; DiFranco et al. 2009) may also contribute to limit the membrane depolarization in response to raised $[K^+]_o$.

On the other hand, the effects of 15 mM K_o^+ on Ca^{2+} transients are different to those produced by a depolarization to the same value measured in the presence of this $[K^+]$ and could not be reversed by current injection. This result suggests that K^+ ions may have an additional (direct) effect on the ECC mechanism. One possible target of K^+ action may be the K^+ inward rectifier. Several lines of evidence give some support to this possibility. The conductance of this channel increases with $[K^+]_o$ (Leech and Stanfield 1981), the space constant of the *t*-tubules is smaller the higher the inward potassium conductance (Schneider and Chandler 1976), and the higher the inward potassium conductance the more attenuated the propagation along the *t*-tubules (Heiny et al. 1983). This intriguing effect of 15 mM K_o^+ has not been reported before. If confirmed by others, it would reveal a new role for the inward potassium conductance, the main muscle potassium conductance at rest.

Further directions

The present work highlights the significance of using cut fibers to study possible factors involved in high frequency fatigue in isolation as an approach to unveil the mechanisms underlying this phenomenon. It also points towards the need of characterizing the *t*-tubule APs and localized Ca^{2+} release during high frequency stimulation. As demonstrated here, the use of current and voltage clamp methods as an alternative to approaches based on field stimulation and membrane potential recording would allow studying independently the impact of changes in ion concentration, membrane potential, charge movement and the features of AP in the generation of muscle fatigue, while preventing the interplay among those factors. For example, the use of voltage clamp paradigms would allow stimulating the fibers with trains of short voltage pulses or simulated action potentials of constant amplitude and duration while the membrane potential is changed.

Acknowledgments This work is part of MQ PhD Thesis. We thank Eng. Victor Di Franco for constructing the voltage clamp and the shutter control unit. We thank Mr. Marino Di Franco Q. for revising the style of the manuscript. This work was partially supported by CONICIT grant S1-805 to MD.

References

Allen DG, Lamb GD et al (2008) Skeletal muscle fatigue: cellular mechanisms. Physiol Rev 88(1):287–332

Balog EM, Fitts RH (1996) Effects of fatiguing stimulation on intracellular Na+ and K+ in frog skeletal muscle. J Appl Physiol 81(2):679–685

Balog EM, Thompson LV et al (1994) Role of sarcolemma action potentials and excitability in muscle fatigue. J Appl Physiol 76(5):2157–2162

Baylor SM, Hollingworth S (2003) Sarcoplasmic reticulum calcium release compared in slow-twitch and fast-twitch fibres of mouse muscle. J Physiol 551(Pt 1):125–138

Bezanilla F, Caputo C et al (1972) Sodium dependence of the inward spread of activation in isolated twitch muscle fibres of the frog. J Physiol 223(2):507–523

Bigland-Ritchie B, Woods JJ (1984) Changes in muscle contractile properties and neural control during human muscular fatigue. Muscle Nerve 7(9):691–699

Bigland-Ritchie B, Jones DA et al (1979) Excitation frequency and muscle fatigue: electrical responses during human voluntary and stimulated contractions. Exp Neurol 64(2):414–427

Blatter LA, Blinks JR (1991) Simultaneous measurement of Ca^{2+} in muscle with Ca electrodes and aequorin. Diffusible cytoplasmic constituent reduces Ca(2+)-independent luminescence of aequorin. J Gen Physiol 98(6):1141–1160

Bouclin R, Charbonneau E et al (1995) Na+ and K+ effect on contractility of frog sartorius muscle: implication for the mechanism of fatigue. Am J Physiol 268(6 Pt 1):C1528–C1536

Cairns SP, Dulhunty AF (1995) High-frequency fatigue in rat skeletal muscle: role of extracellular ion concentrations. Muscle Nerve 18(8):890–898

Cairns SP, Lindinger MI (2008) Do multiple ionic interactions contribute to skeletal muscle fatigue? J Physiol 586(Pt 17):4039–4054

Cairns SP, Flatman JA et al (1995) Relation between extracellular [K+], membrane potential and contraction in rat soleus muscle: modulation by the Na+ –K+ pump. Pflugers Arch 430(6):909–915

Cairns SP, Hing WA et al (1997) Different effects of raised [K+]o on membrane potential and contraction in mouse fast- and slow-twitch muscle. Am J Physiol 273(2 Pt 1):C598–C611

Cairns SP, Buller SJ et al (2003) Changes of action potentials and force at lowered [Na+]o in mouse skeletal muscle: implications for fatigue. Am J Physiol Cell Physiol 285(5):C1131–C1141

Cairns SP, Chin ER et al (2007) Stimulation pulse characteristics and electrode configuration determine site of excitation in isolated mammalian skeletal muscle: implications for fatigue. J Appl Physiol 103(1):359–368

Cairns SP, Taberner AJ et al (2009) Changes of surface and t-tubular membrane excitability during fatigue with repeated *tetani* in isolated mouse fast- and slow-twitch muscle. J Appl Physiol 106(1):101–112

Caputo C, Fernandez de Bolanos P (1979) Membrane potential, contractile activation and relaxation rates in voltage clamped short muscle fibres of the frog. J Physiol 289:175–189

Caputo C, Edman KA et al (1994) Variation in myoplasmic Ca^{2+} concentration during contraction and relaxation studied by the indicator fluo-3 in frog muscle fibres. J Physiol 478(Pt 1):137–148

Caputo C, Bolanos P, Escobar AL (1999) Fast calcium removal during single twitches in amphibian skeletal muscle fibres. J Muscle Res Cell Motil 20(5–6):555–567

Clausen T (2008) Clearance of extracellular K+ during muscle contraction–roles of membrane transport and diffusion. J Gen Physiol 131(5):473–481

Clausen T, Nielsen OB (2008) Increased interstitial K+ as a cause of muscle fatigue: response to a Letter to the Editor. J Physiol 586:1209

Coonan JR, Lamb GD (1998) Effect of transverse-tubular chloride conductance on excitability in skinned skeletal muscle fibres of rat and toad. J Physiol 509(Pt 2):551–564

DiFranco M (1991) Medición cuantitativa de la concentración de calcio en fibras musculares esqueléticas. Ph.D. Thesis, Caracas, Universidad Central de Venezuela

DiFranco M, Quinonez M et al. (2009) DNA transfection of mammalian skeletal muscles using in vivo electroporation. J Vis Exp 32:1520

DiFranco M, Quinonez M et al (1999) Inverted double-gap isolation chamber for high-resolution calcium fluorimetry in skeletal muscle fibers. Pflugers Arch 438(3):412–418

DiFranco M, Novo D et al (2002) Characterization of the calcium release domains during excitation-contraction coupling in skeletal muscle fibres. Pflugers Arch 443(4):508–519

DiFranco M, Capote J et al (2005) Optical imaging and functional characterization of the transverse tubular system of mammalian muscle fibers using the potentiometric indicator di-8-ANEPPS. J Membr Biol 208(2):141–153

DiGregorio DA, Peskoff A et al (1999) Measurement of action potential-induced presynaptic calcium domains at a cultured neuromuscular junction. J Neurosci 19(18):7846–7859

Dutka TL, Lamb GD (2007) Transverse tubular system depolarization reduces tetanic force in rat skeletal muscle fibers by impairing action potential repriming. Am J Physiol Cell Physiol 292(6):C2112–C2121

Duty S, Allen DG (1994) The distribution of intracellular calcium concentration in isolated single fibres of mouse skeletal muscle during fatiguing stimulation. Pflugers Arch 427(1–2):102–109

Edwards RH (1981) Human muscle function and fatigue. Ciba Found Symp 82:1–18

Escobar AL, Velez P et al (1997) Kinetic properties of DM-nitrophen and calcium indicators: rapid transient response to flash photolysis. Pflugers Arch 434(5):615–631

Fitts RH (1994) Cellular mechanisms of muscle fatigue. Physiol Rev 74(1):49–94

Fitts RH (1996) Muscle fatigue: the cellular aspects. Am J Sports Med 24(6 Suppl):S9–S13

Fitts RH, Balog EM (1996) Effect of intracellular and extracellular ion changes on E-C coupling and skeletal muscle fatigue. Acta Physiol Scand 156(3):169–181

Frankenhaeuser B, Lannergren J (1967) The effect of calcium on the mechanical response of single twitch muscle fibres of *Xenopus laevis*. Acta Physiol Scand 69(3):242–254

Gonzalez-Serratos H, Somlyo AV et al (1978) Composition of vacuoles and sarcoplasmic reticulum in fatigued muscle: electron probe analysis. Proc Natl Acad Sci USA 75(3):1329–1333

Grabowski W, Lobsiger EA et al (1972) The effect of repetitive stimulation at low frequencies upon the electrical and mechanical activity of single muscle fibres. Pflugers Arch 334(3):222–239

Heiny JA, Ashcroft FM et al (1983) T-system optical signals associated with inward rectification in skeletal muscle. Nature 301(5896):164–166

Hollingworth S, Soeller C et al (2000) Sarcomeric Ca^{2+} gradients during activation of frog skeletal muscle fibres imaged with confocal and two-photon microscopy. J Physiol 526(Pt 3):551–560

Holmberg E, Waldeck B (1980) On the possible role of potassium ions in the action of terbutaline on skeletal muscle contractions. Acta Pharmacol Toxicol (Copenh) 46(2):141–149

Huang CL (1981) Dielectric components of charge movements in skeletal muscle. J Physiol 313:187–205

Huang CL (1994) Kinetic separation of charge movement components in intact frog skeletal muscle. J Physiol 481(Pt 2):357–369

Juel C (1986) Potassium and sodium shifts during in vitro isometric muscle contraction, and the time course of the ion-gradient recovery. Pflugers Arch 406(5):458–463

Juel C, Pilegaard H et al (2000) Interstitial K(+) in human skeletal muscle during and after dynamic graded exercise determined by microdialysis. Am J Physiol Regul Integr Comp Physiol 278(2):R400–R406

Kristensen M, Juel C (2009) Potassium-transporting proteins in skeletal muscle: cellular location and fiber-type differences. Acta Physiol (Oxf)

Kurebayashi N, Harkins AB et al (1993) Use of fura red as an intracellular calcium indicator in frog skeletal muscle fibers. Biophys J 64(6):1934–1960

Lannergren J, Westerblad H (1986) Force and membrane potential during and after fatiguing, continuous high-frequency stimulation of single Xenopus muscle fibres. Acta Physiol Scand 128(3):359–368

Lee JA, Westerblad H et al (1991) Changes in tetanic and resting $[Ca^{2+}]$i during fatigue and recovery of single muscle fibres from *Xenopus laevis*. J Physiol 433:307–326

Leech CA, Stanfield PR (1981) Inward rectification in frog skeletal muscle fibres and its dependence on membrane potential and external potassium. J Physiol 319:295–309

Lopez JR, Alamo L et al (1983) Determination of ionic calcium in frog skeletal muscle fibers. Biophys J 43(1):1–4

Lynch GS, Fary CJ et al (1997) Quantitative measurement of resting skeletal muscle $[Ca^{2+}]$i following acute and long-term downhill running exercise in mice. Cell Calcium 22(5):373–383

Neuhaus R, Rosenthal R et al (1990) The effects of dihydropyridine derivatives on force and Ca^{2+} current in frog skeletal muscle fibres. J Physiol 427:187–209

Nordsborg N, Mohr M et al (2003) Muscle interstitial potassium kinetics during intense exhaustive exercise: effect of previous arm exercise. Am J Physiol Regul Integr Comp Physiol 285(1):R143–R148

Place N (2008) Is interstitial K + accumulation a key factor in the fatigue process under physiological conditions? J Physiol 586(4):1207–1208 author reply 1209

Prosser BL, Hernandez-Ochoa EO et al (2009a) The Qgamma component of intra-membrane charge movement is present in mammalian muscle fibres, but suppressed in the absence of S100A1. J Physiol 587(Pt 18):4523–4541

Prosser BL, Hernandez-Ochoa EO et al (2009b) Simultaneous recording of intramembrane charge movement components and calcium release in wild-type and S100A1−/− muscle fibres. J Physiol 587(Pt 18):4543–4559

Quinonez M, DiFranco M (2000) Novel inverted triple grease-gap isolation chamber for electrophysiological and calcium release studies in skeletal muscle fibers. Jpn J Physiol 50(4):457–462

Quiñonez M, González F et al (2009) Effects of changes in extracellular concentration of Na+ and K+ ([Na+]o, [K+]o) on the Ca^{2+} release elicited by high frequency stimulation. Implications for muscle fatigue. Biophys J 96(3):233a–234a

Renaud JM, Light P (1992) Effects of K+ on the twitch and tetanic contraction in the sartorius muscle of the frog, *Rana pipiens*. Implication for fatigue in vivo. Can J Physiol Pharmacol 70(9):1236–1246

Rios E, Pizarro G et al (1992) Charge movement and the nature of signal transduction in skeletal muscle excitation-contraction coupling. Annu Rev Physiol 54:109–133

Sanchez JA, Vergara J (1994) Modulation of Ca^{2+} transients by photorelease of caged nucleotides in frog skeletal muscle fibers. Am J Physiol 266(5 Pt 1):C1291–C1300

Schneider MF, Chandler WK (1976) Effects of membrane potential on the capacitance of skeletal muscle fibers. J Gen Physiol 67(2):125–163

Shorten PR, O'Callaghan P et al (2007) A mathematical model of fatigue in skeletal muscle force contraction. J Muscle Res Cell Motil 28(6):293–313

Sjogaard G, Adams RP et al (1985) Water and ion shifts in skeletal muscle of humans with intense dynamic knee extension. Am J Physiol 248(2 Pt 2):R190–R196

Snowdowne KW (1985) Subcontracture depolarizations increase sarcoplasmic ionized calcium in frog skeletal muscle. Am J Physiol 248(5 Pt 1):C520–C526

Westerblad H, Allen DG (1993) The contribution of $[Ca^{2+}]$i to the slowing of relaxation in fatigued single fibres from mouse skeletal muscle. J Physiol 468:729–740

Westerblad H, Allen DG (2003) Cellular mechanisms of skeletal muscle fatigue. Adv Exp Med Biol 538:563–570 discussion 571

Westerblad H, Lee JA et al (1990) Spatial gradients of intracellular calcium in skeletal muscle during fatigue. Pflugers Arch 415(6):734–740

Westerblad H, Lee JA et al (1991) Cellular mechanisms of fatigue in skeletal muscle. Am J Physiol 261(2 Pt 1):C195–C209

Yensen C, Matar W et al (2002) K+ -induced twitch potentiation is not due to longer action potential. Am J Physiol Cell Physiol 283(1):C169–C177